

Integrative Analysis of the Acquisition of Pluripotency in PGCs Reveals the Mutually Exclusive Roles of Blimp-1 and AKT Signaling

Go Nagamatsu,^{1,2,3,*} Shigeru Saito,⁴ Keiyo Takubo,^{1,5} and Toshio Suda^{1,6,7}

¹Department of Cell Differentiation, The Sakaguchi Laboratory, School of Medicine, Keio University, Tokyo 160-8582, Japan

²Precursory Research for Embryonic Science and Technology, Japan Science and Technology Agency, Kawaguchi, Saitama 332-0012, Japan

³Department of Stem Cell Biology and Medicine, Graduate School of Medical Science, Kyushu University, Fukuoka 812-8582, Japan

⁴Data Science Lab, OPT, Tokyo 102-0081, Japan

⁵Department of Stem Cell Biology, Research Institute, National Center for Global Health and Medicine, Tokyo 162-8655, Japan

⁶Cancer Science Institute (CSI), National University of Singapore (NUS), 14 Medical Drive, Singapore 117599, Singapore

⁷International Research Center for Medical Sciences (IRCMS), Kumamoto University, Kumamoto, 860-0811, Japan

*Correspondence: gonag@hgs.med.kyushu-u.ac.jp

<http://dx.doi.org/10.1016/j.stemcr.2015.05.007>

This is an open access article under the CC BY-NC-ND license (<http://creativecommons.org/licenses/by-nc-nd/4.0/>).

SUMMARY

Primordial germ cells (PGCs) are lineage-restricted unipotent cells that can dedifferentiate into pluripotent embryonic germ cells (EGCs). Here we performed whole-transcriptome analysis during the conversion of PGCs into EGCs, a process by which cells acquire pluripotency. To examine the molecular mechanism underlying this conversion, we focused on *Blimp-1* and *Akt*, which are involved in PGC specification and dedifferentiation, respectively. *Blimp-1* overexpression in embryonic stem cells suppressed the expression of downstream targets of the pluripotency network. Conversely, *Blimp-1* deletion in PGCs accelerated their dedifferentiation into pluripotent EGCs, illustrating that *Blimp-1* is a pluripotency gatekeeper protein in PGCs. AKT signaling showed a synergistic effect with basic fibroblast growth factor plus 2i+A83 treatment on EGC formation. AKT played a major role in suppressing genes regulated by MBD3. From these results, we defined the distinct functions of *Blimp-1* and *Akt* and provided mechanistic insights into the acquisition of pluripotency in PGCs.

INTRODUCTION

Germ cells are the only cells that continue to be reprogrammed throughout their lifetime in order to transfer genetic information to subsequent generations (Sasaki and Matsui, 2008). Germ cells have unique characteristics such as genome-wide epigenetic reprogramming and the potential to become pluripotent (Saitou and Yamaji, 2012). Primordial germ cells (PGCs) are specified at embryonic day (E) 7 in the epiblast. *Blimp-1*, *Prdm14*, and *Tfap2c* have critical roles in the specification of PGCs. A functional study of knockout embryos showed that BLIMP-1 represses somatic genes (Ohinata et al., 2005), whereas PRDM14 activates germ cell development genes (Yamaji et al., 2008). *Tfap2c* is thought to be a functional downstream target of BLIMP-1 (Weber et al., 2010). These three factors are sufficient to induce PGCs in vitro (Nakaki et al., 2013). Germ cell development, especially PGC specification, shares similarities with somatic cell reprogramming. Factors involved in germ cell development also function in the reprogramming of somatic cells (Nagamatsu et al., 2011). Moreover, PGCs have the potential to dedifferentiate into pluripotent embryonic germ cells (EGCs) without exogenous gene activation (Matsui et al., 1992). Although pluripotent stem cells and PGCs share many common features, PGCs are unipotent germ lineage-restricted cells and are distinct from pluripotent stem cells. When injected into blastocysts, PGCs do not give rise to any cell lineages (Leitch et al., 2014).

Originally, EGCs were established through screening of the culture conditions required for PGC proliferation (Matsui et al., 1992). Basic fibroblast growth factor (bFGF), leukemia inhibitory factor (LIF), and membrane-bound stem cell factor (mSCF) are present under these culture conditions. Because activation of phosphoinositide-3-kinase and AKT signaling negates the requirement for bFGF in such cultures, *Akt* is known to be involved in the induction of pluripotency in PGCs (Kimura et al., 2008). Recently, it was reported that a combination of signaling inhibitors enhances the efficiency of EGC formation (Leitch et al., 2010; Nagamatsu et al., 2012a). These inhibitors consist of 2i inhibitors (inhibitors of mitogen-activated protein kinase kinase [MEK] and glycogen synthase kinase- β), which maintain pluripotency, and A83 (an inhibitor of transforming growth factor- β receptor), which enhances somatic cell reprogramming (Ying et al., 2008; Yuan et al., 2011). However, the mechanisms underlying the induction of pluripotency in PGCs remain largely elusive. While only germ cells can give rise to pluripotent cells following implantation, induced pluripotent stem cell (iPSC) technology enables pluripotent cells to be established from somatic cells (Takahashi and Yamanaka, 2006). Methyl-CpG binding domain protein 3 (Mbd3) was recently identified as a roadblock of somatic cell reprogramming (Rais et al., 2013). MBD3 is a component of the nucleosome remodeling deacetylase (NuRD) complex, which has histone



deacetylase activity and serves to close the chromatin structure (Hu and Wade, 2012).

In this study, we performed extensive gene expression analysis during the dedifferentiation of PGCs into EGCs and combined these data with the data for previously published target gene sets. Extensive analysis of transcription profiles revealed that BLIMP-1 suppressed pluripotency network genes and was therefore a pluripotency gatekeeper protein in PGCs. Moreover, there was a synergistic effect of AKT activation in the presence of bFGF and 2i+A83 on EGC formation. AKT activation suppressed genes regulated by MBD3. The targets of AKT and BLIMP-1 were different. Taken together, these results provide insight into the mechanism by which PGCs are converted into EGCs.

RESULTS

Transcriptome Analysis during the Conversion of PGCs into Pluripotent Stem Cells

To elucidate the molecular mechanisms by which PGCs become pluripotent cells, we performed whole-transcriptome analysis during the conversion of PGCs into EGCs. To obtain precise data, we used specific culture conditions for purified pluripotent candidate cells as previously reported (Figure 1A) (Nagamatsu and Suda, 2013). Heatmap and principal component analysis (PCA) indicated that the acquisition of pluripotency in PGCs is a stepwise process (Figures 1B and 1C). Table S1 shows the various genes that are gradually upregulated and downregulated during the conversion process. Gene Ontology (GO) analysis indicated that the transcription of genes involved in processes such as “transcription, DNA-dependent” and “regulation of transcription, DNA-dependent” was upregulated, while the transcription of genes involved in “protein-chromosome linkage” was downregulated (Table S1). To understand the global changes in gene expression during the acquisition of pluripotency, we compared the numbers of differentially expressed genes at each time point of the culture (Figure 1D). There were two waves observed by differentially expressed genes. The first wave was from day 0 to day 1, and the second wave was from day 6 to day 10. When these differentially expressed genes were divided into upregulated or downregulated genes, most genes in the first wave were upregulated, and most genes in the second wave were downregulated (Figure 1E). Moreover, more than half of the genes upregulated in the first wave were downregulated in the second wave (Figure 1F; Table S1), indicating that they were oppositely regulated during these time periods. When we focused on these genes, GO analysis revealed the enrichment of terms associated with the “cell cycle,” “development,” and “metabolism” (Table S1).

Next, we analyzed the characteristic gene expression of PGCs. Gene set enrichment analysis (GSEA) showed that PGC markers were downregulated from day 2 of the culture (Figure 1G). This indicated that the PGC characteristics were lost in the early phase of pluripotency acquisition.

Analysis of the Core Transcription Network Involved in the Conversion of PGCs into Pluripotent Stem Cells

To analyze gene expression in pluripotent candidate cells (Nagamatsu et al., 2012a), we focused on downstream targets of the core transcription network (Kim et al., 2008). Because PGCs express key transcription factors of pluripotent stem cells, such as *Oct3/4*, *Sox2*, and *Nanog* (Nagamatsu et al., 2013), it would be difficult to understand the differences between pluripotent stem cells and PGCs from the expression of these key factors themselves. In fact, with the exception of *Dax1*, the expression levels of the key pluripotency core network did not fluctuate during the acquisition of pluripotency (Figure S1). Therefore, we focused on the gene expression changes in the downstream targets of the core transcription network. We collected target gene sets from previous reports and applied these data to the GSEA of our time course gene expression profiles (Figure 2A) (Kim et al., 2008). Whereas the target genes of OCT3/4 tended to be repressed until EGCs formed, the targets of other core network factors were maintained or gradually upregulated during the conversion of PGCs into EGCs (Figure 2A). To evaluate the changes of this network, we calculated the numbers of genes commonly regulated by various network factors (Figure 2B). Some of these commonly regulated genes were involved in the process of pluripotency acquisition. Genes regulated by multiple factors of the core network are generally active in embryonic stem cells (ESCs), and these factors may be important in self-renewal and lineage commitment (Kim et al., 2008; Jeong et al., 2001). Therefore, we focused on genes that shared more than seven of nine regulatory factors in common (Table S2). Most of these genes that were activated in the early stage of the culture were also implicated in the late stage. Seven of ten genes involved in both the early (before day 3) and late (after day 6) culture stages encoded DNA-binding proteins involved in the control of transcription and/or chromatin remodeling (*Klf9*, *Dido1*, *Rarg*, *Trim8*, *Mybl2*, *Zfp207*, and *Chd9*). Such factors might function as a hub for the gene expression of other components of the core network.

The PGC-Specific Gene Blimp-1 Represses Downstream Targets of Pluripotency Network Genes

Microarray data of the conversion of PGCs into EGCs revealed an inverse correlation between certain PGC characteristics and pluripotent characteristics. We speculated that there is a mechanism that suppresses pluripotent

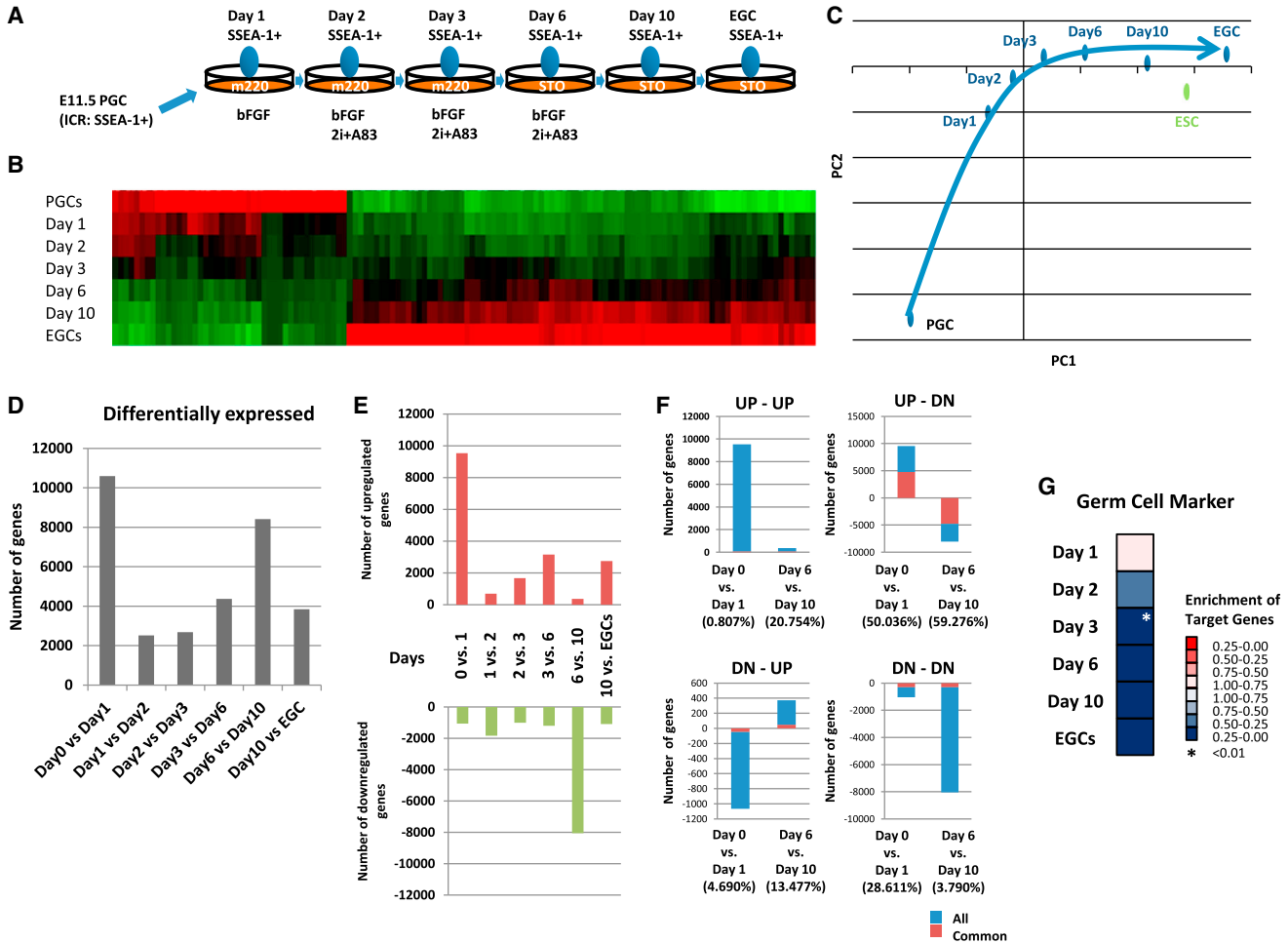


Figure 1. Microarray Analysis of the Acquisition of Pluripotency in PGCs

(A) Summary of the procedure used to culture cells and isolate samples. Gonads were surgically isolated from E11.5 embryos. After making a single cell suspension, PGCs were isolated based on SSEA-1 expression using a FACS AriaII cell sorter. Purified PGCs were seeded onto m220 feeder cells in ESC medium containing bFGF. One day after seeding, 2i+A83 was added to the culture. At day 3 of culture, the cells were reseeded onto STO feeder cells. At day 7 of culture, bFGF and 2i+A83 were removed by changing the medium. Colonies were picked, and EGC lines were established. At each time point, pluripotent candidate cells were sorted based on stage-specific embryonic antigen-1 (SSEA-1) expression for microarray analysis (Nagamatsu and Suda, 2013). 2i+A83 was composed of inhibitors of MEK (PD325901), glycogen synthase kinase- β (CHIR99021), and transforming growth factor- β type 1R (A83-01).

(B) Array heatmap of differentially expressed genes according to the culture period.

(C) Principle component analysis during the acquisition of pluripotency in PGCs.

(D) The number of differentially expressed genes at each adjacent time point.

(E) The numbers of upregulated and downregulated genes at each adjacent time point.

(F) The numbers of oppositely regulated genes at day 0 versus day 1 and day 6 versus day 10 during the acquisition of pluripotency. The bars indicate the total number of genes at each time point. Red indicates common genes at day 0 versus day 1 or day 6 versus day 10. The percentage of common genes is shown below each bar. DN, downregulated; UP, upregulated.

(G) GSEA of the PGC markers.

See also Table S1.

characteristics in PGCs. To investigate this possibility, we performed microarray analysis of ESCs, which expressed each germ gene. First, we selected six genes that are preferentially expressed in PGCs rather than in ESCs, namely, *Prdm14*, *Vasa*, *Nanos2*, *Nanos3*, *Dnd*, and *Blimp-1* (Figure 3A)

(Yamaji et al., 2008; Tanaka et al., 2000; Suzuki et al., 2007, 2008; Youngren et al., 2005; Ohinata et al., 2005). We generated ESCs that expressed PGC genes under the control of doxycycline (Masui et al., 2005). We could not obtain a stable clone of inducible *Blimp-1*-expressing

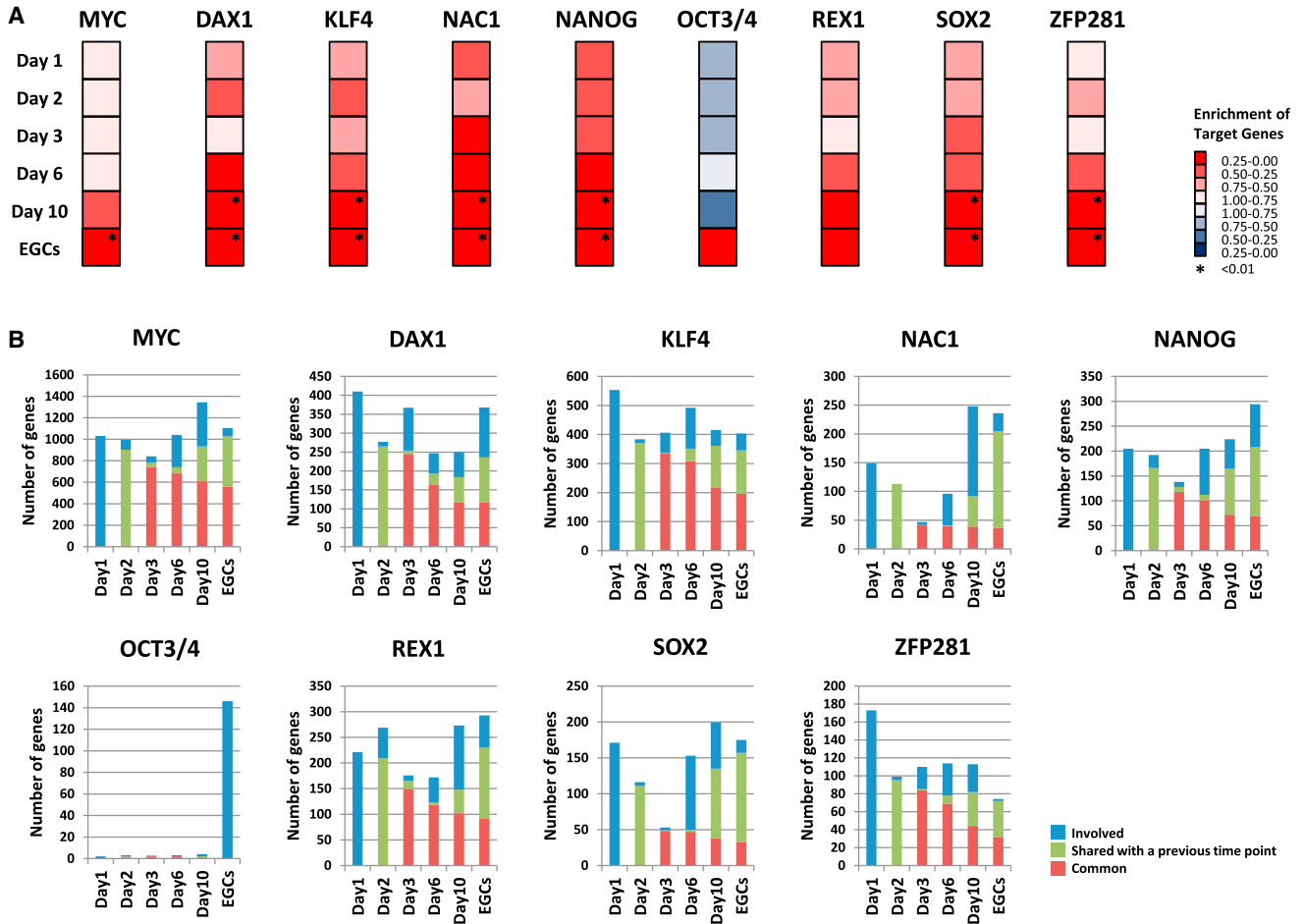


Figure 2. GSEA of Downstream Targets

(A) GSEA of downstream targets of the pluripotency network from Kim et al. (2008).

(B) The numbers of involved genes (blue), genes shared with a previous time point (green), and common genes (red) of the GSEA.

See also Figure S1 and Table S2.

ESCs; therefore, *Blimp-1*-overexpressing cells were analyzed by transfection of ESCs with the *Blimp-1-IRES-AcGFP* vector and sorting of GFP-positive cells by fluorescence-activated cell sorting (FACS). Gene expression levels were confirmed by RT-PCR (Figure 3B). Microarray data were integrated with previously reported pluripotency network targets as shown in Figure 2A. *Prdm14* is essential for germ cell specification and the maintenance of ESC pluripotency (Yamaji et al., 2013). When *Prdm14* was overexpressed in ESCs, downstream targets of the pluripotency network were activated (Figure 3C). Similarly, expression of the other four germ cell-specific genes (*Vasa*, *Nanos2*, *Nanos3*, and *Dnd*) activated these downstream targets (Figure 3C). However, when *Blimp-1* was overexpressed in ESCs, the downstream targets were clearly repressed (Figure 3C). These results suggest that pluripotency suppression is not achieved by the cooperation of multiple germ cell factors; rather, *Blimp-1*

appears to function as a pluripotency gatekeeper protein in PGCs.

Identification of a *Blimp-1* Module in ESCs

To understand the mechanism by which BLIMP-1 suppresses downstream targets of the pluripotency network, we attempted to identify BLIMP-1 targets in ESCs. Recently, BLIMP-1-regulated genes were identified by chromatin immunoprecipitation (ChIP)-sequencing analysis of BLIMP-1 in PC19 pluripotent embryonic carcinoma cells (Magnúsdóttir et al., 2013). These BLIMP-1-regulated genes were projected to pluripotency controlling modules of CoORE, Polycomb (PRC), and MYC (Kim et al., 2010). In total, 4,808 unique genes were identified from BLIMP-1 ChIP-sequencing analysis and were included in the modules. We referred to these putative BLIMP-1 targets in ESCs as the BLIMP-1 modules (Figure 4A). Among the

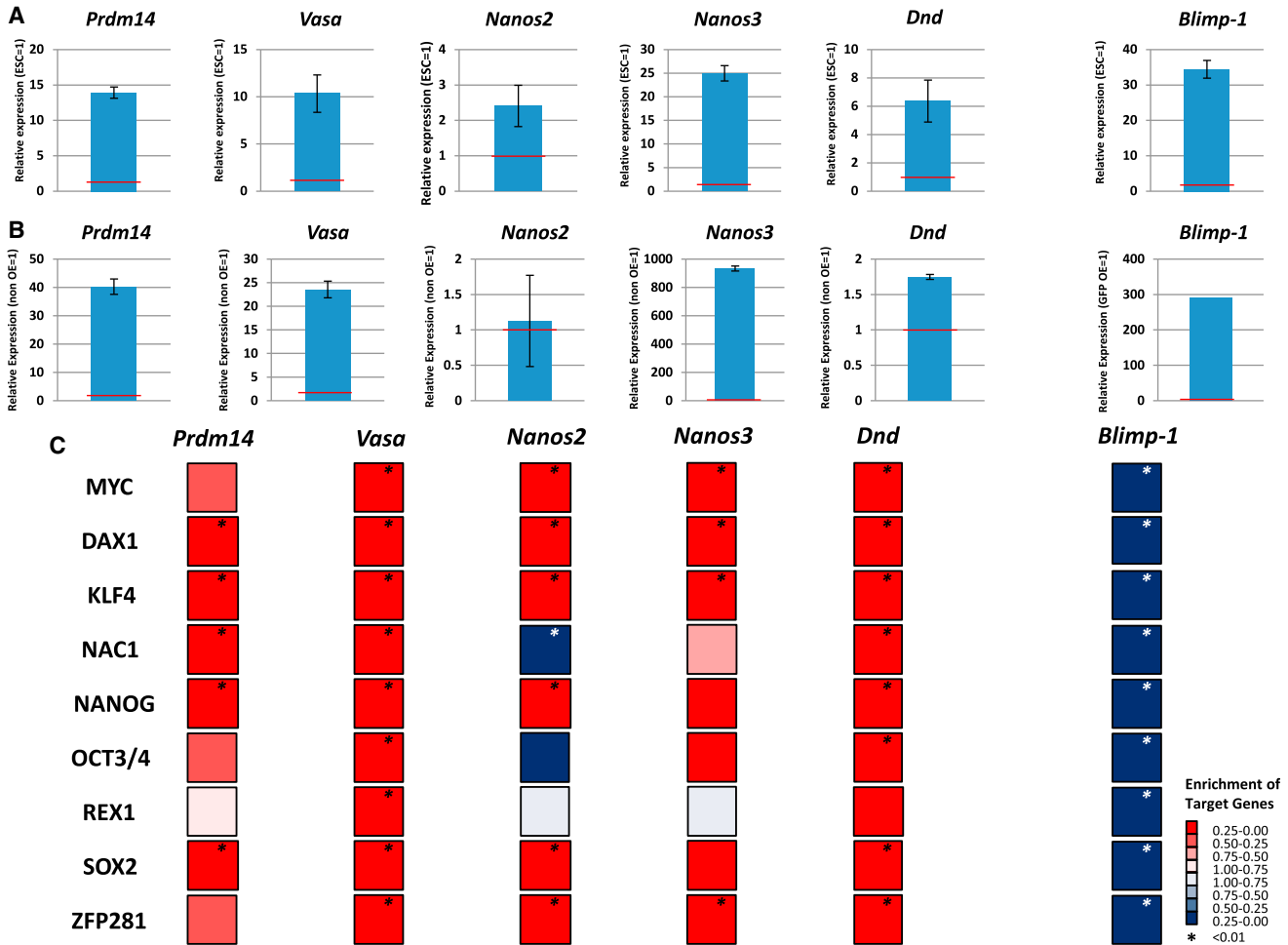


Figure 3. Blimp-1 Represses Downstream Targets of Pluripotency Network Genes

(A) Gene expression of the germ cell markers is shown. Expression in E11.5 PGCs was compared with that in ESCs (TT2). Relative gene expression is shown (mean \pm SD; independent experiments, $n = 3$). Red bars indicate the expression level in ESCs (set at 1).

(B) Gene expression of germ cell markers in ESCs. The expression in overexpressing ESCs was compared with that in parental ESCs. Relative gene expression is shown (mean \pm SD; independent experiments, $n = 3$). Red bars indicate the expression level in parental ESCs (set at 1). In the case of *Blimp-1*, expression in ESCs transfected with *Blimp-1-IRES-AcGFP* was compared with that in ESCs transfected with *IRES-AcGFP*. Red bars indicate the expression level in ESCs transfected with *IRES-AcGFP* (set at 1).

(C) GSEA of downstream targets of the pluripotency network from Kim et al. (2008). ESCs overexpressing each germ cell gene were compared with parental ESCs. In the case of *Blimp-1*, ESCs were transfected with *pEF1 α -IRES-AcGFP* or *EF1 α -Blimp-1-IRES-AcGFP*, and then AcGFP-positive cells were sorted and compared.

CORE, PRC, and MYC modules, about 40% of genes belonged to the BLIMP-1 module (Figures 4B and 4C). Next, the BLIMP-1 module was applied to our microarray data from *Blimp-1*-overexpressing ESCs. When *Blimp-1* was overexpressed in ESCs, the majority of BLIMP-1 module genes were downregulated, while about 10% of genes were upregulated (Figure 4D). Most of these upregulated genes were collectively classified as a PRC module (Figures 4E–4G). In ESCs, whereas CORE and MYC modules are activated, PRC modules are suppressed (Kim et al., 2010).

Therefore, *Blimp-1* likely suppressed pluripotency through a BLIMP-1 module.

Blimp-1 Depletion Induces Pluripotency in PGCs

To clarify the functional role of *Blimp-1* in pluripotency acquisition in PGCs, we deleted *Blimp-1*. First, we purified PGCs from *Blimp-1*-floxed mouse embryos and then used recombinant CRE protein to delete *Blimp-1* (Ohinata et al., 2005). CRE-treated PGCs were seeded onto STO or m220 feeder cells without bFGF. In the absence of bFGF,

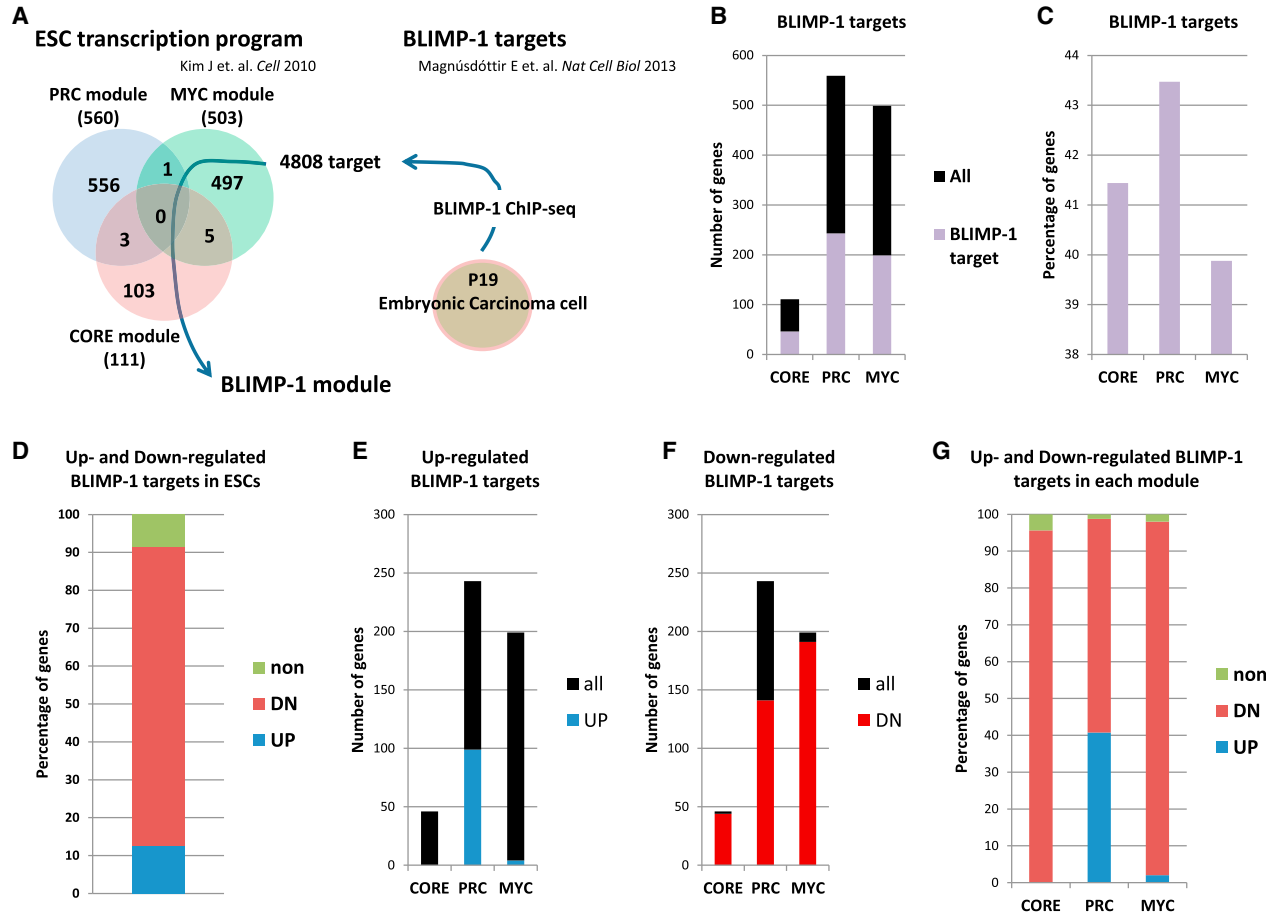


Figure 4. Identification of Blimp-1 Modules in ESCs

(A) Summary of the identification of BLIMP-1 modules in ESCs. BLIMP-1 targets were obtained from the ChIP-sequencing data of Magnúsdóttir et al. (2013) (right). The 4808 BLIMP-1-regulated genes targets were projected to each regulated module of ESCs reported by Kim et al. (2010) (left). These overlapped genes were identified as individual BLIMP-1 modules.

(B) The numbers of BLIMP-1 target genes in each regulated module of ESCs.

(C) Percentage of BLIMP-1 target genes in each regulated module of ESCs.

(D) Percentage of upregulated and downregulated BLIMP-1 targets in ESCs at day 2.

(E) Numbers of upregulated genes in each BLIMP-1 module in *Blimp-1*-overexpressing ESCs at day 2.

(F) Numbers of downregulated genes in each BLIMP-1 module in *Blimp-1*-overexpressing ESCs at day 2.

(G) Percentage of upregulated and downregulated genes in each BLIMP-1 module in *Blimp-1*-overexpressing ESCs at day 2. DN, down-regulated; UP, upregulated.

PGCs could not convert to EGCs (Durcova-Hills et al., 2006). m220 feeder cells express mSCF, which is an important signal for EGC formation (Matsui et al., 1992). After culture, ESC-like colonies formed from *Blimp-1*-deleted PGCs grown on both types of feeder cells (Figures 5A–5C). *Blimp-1* deletion was confirmed by genomic PCR (Figure S2A). Additional treatment with 2i+A83, which enhances EGC generation (Nagamatsu et al., 2012a), also enhanced the efficiency with *Blimp-1* deletion. On the other hand, in the presence of bFGF, the efficiency was decreased. These results indicated that there is no synergistic effect between *Blimp-1* deletion and bFGF. The gene

expression pattern in *Blimp-1*-deleted ESC-like colony cells indicated that the lack of *Blimp-1* induced the upregulation of *Klf4* and *ERas* (Figure 5D). When injected into nude mice, these established ESC-like cells formed teratomas containing three germ layers (Figures 5E and 5F), reminiscent of pluripotent stem cells. These results indicate that *Blimp-1* deletion causes PGCs to becoming pluripotent. In the next experiment, rather than deleting *Blimp-1*, we induced the forced expression of *Blimp-1* in PGCLCs during EGC formation. PGCLCs are in vitro-induced PGCs from ESCs (Hayashi et al., 2011). In this study, we established these cells using doxycycline inducible *Blimp-1*-expressing

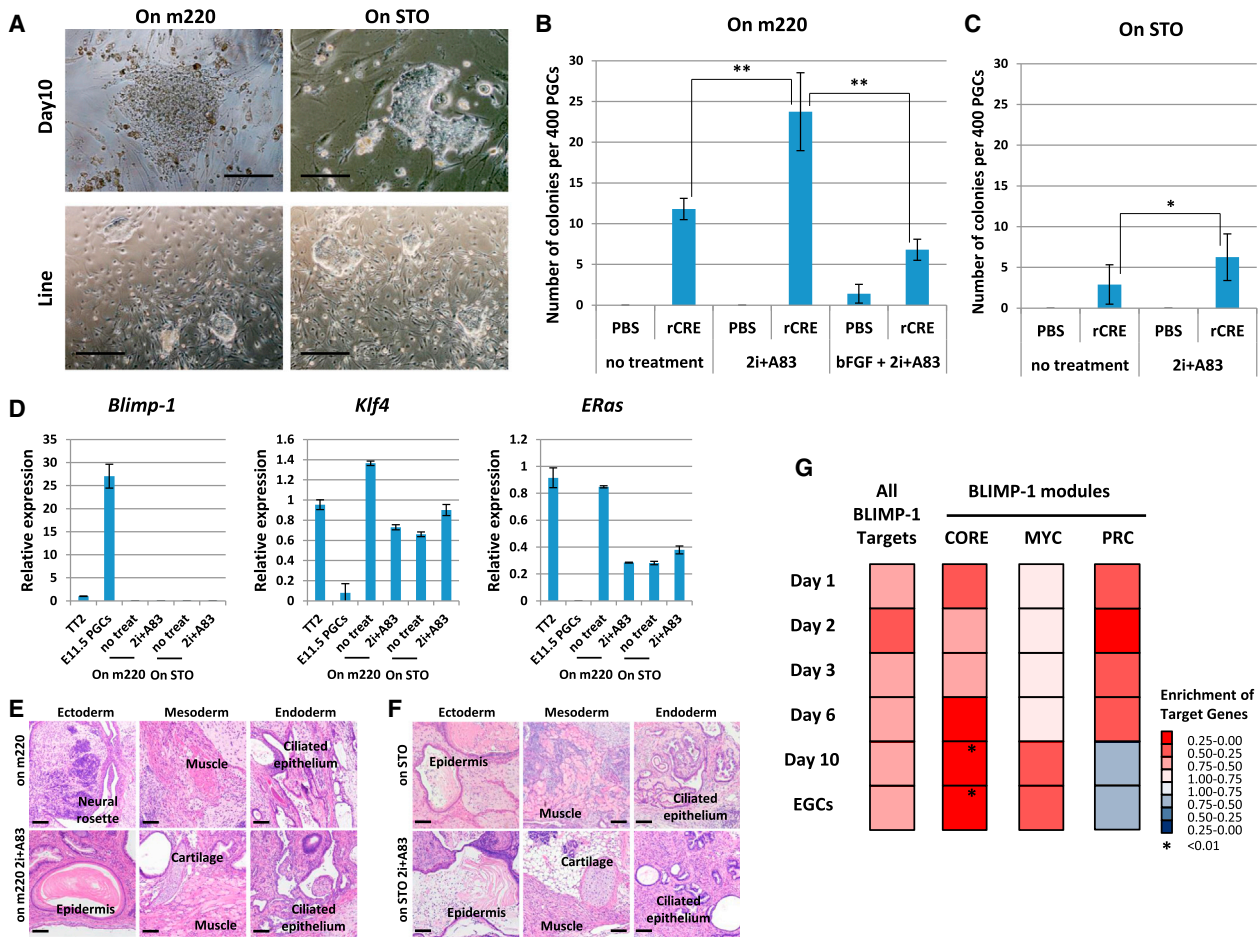


Figure 5. Blimp-1 Depletion Induces Pluripotency in PGCs

(A) Typical morphology of embryonic stem cell (ESC)-like colonies after *Blimp-1* depletion by CRE treatment and culture on feeder cells (m220 or STO). A primary colony at day 10 of culture and an established line are shown. Scale bars 100 μ m (top) and 500 μ m (bottom). (B and C) The number of ESC-like colonies observed 10 days after *Blimp-1* deletion by CRE treatment and culture on m220 (B) or STO (C) feeder cells with or without 2i+A83 treatment. Data represent the mean \pm SD of independent experiment. Statistical significance was determined using Tukey's multiple comparison test ($n = 5$ for no treatment on m220, $n = 4$ for 2i+A83 on m220, $n = 5$ for bFGF + 2i+A83, $n = 10$ for no treatment on STO and $n = 4$ for 2i+A83 on STO). ** $p < 0.01$, * $p = 0.019$.

(D) Gene expression analyses of *Blimp-1*-depleted EGCs for *Blimp-1* (left), *Klf4* (middle), and *ERas* (right) are shown (mean \pm SD; independent experiments, $n = 3$).

(E and F) Teratoma formation by *Blimp-1*-depleted EGCs induced on m220 (E) or STO (F) feeder cells, with or without 2i+A83 treatment. Scale bars represent 50 μ m.

(G) GSEA of BLIMP-1 targets for the microarray time course data. BLIMP-1 modules are the gene sets identified in Figure 4. rCRE, recombinant CRE.

See also Figure S2.

ESCs (Nakaki et al., 2013). When *Blimp-1* was induced at the early phase of the EGC formation, PGCLCs could not convert to EGCs (Figure S2B). To confirm the effect of BLIMP-1 modules during the acquisition of pluripotency in PGCs, we analyzed expression changes of BLIMP-1 modules in the time course transcriptome data. Whereas the BLIMP-1 modules of CORE and MYC were activated, the BLIMP-1 module of PRC was suppressed (Figure 5G). These changes correspond to the regulation in ESCs, suggesting

that the BLIMP-1 modules are of functional relevance during EGC formation (Kim et al., 2010). Taken together, these results show that *Blimp-1* acted as a gatekeeper of pluripotency in PGCs.

AKT Has a Synergistic Effect with bFGF and 2i+A83 on the Acquisition of Pluripotency

Next, we analyzed the key signaling required for the acquisition of pluripotency in PGCs. Whereas bFGF is an

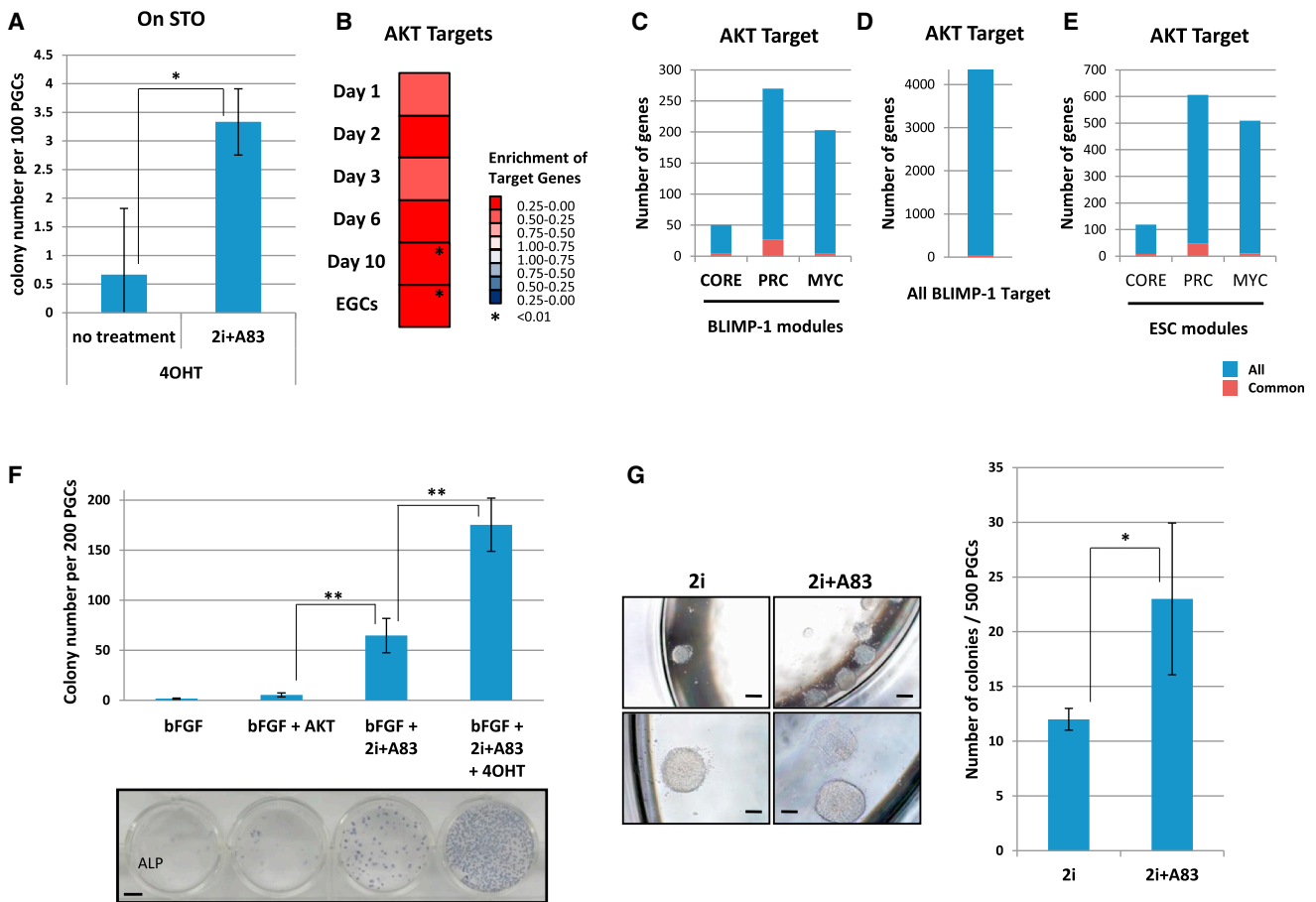


Figure 6. Synergistic Effect of AKT Activation Together with bFGF and 2i+A83 Treatment

(A) E11.5 PGCs were purified based on SSEA-1 expression. PGCs were seeded onto STO feeder cells in ESC medium containing 4-hydroxytamoxifen (4OHT) with or without 2i+A83. The numbers of ESC-like colonies at day 10 are shown. Data represent the mean \pm SD of independent experiments. Statistical significance was determined using Student's t test ($n = 3$). * $p = 0.047$.

(B) GSEA of AKT targets for the microarray time course data. AKT targets were identified by comparison with the data of Yamano et al. (2010).

(C) Number of AKT targets in Blimp-1 modules. The bars indicate the total number of genes in each Blimp-1 module (Figure 4A). Red indicates AKT target genes.

(D) Number of AKT targets among all BLIMP-1 targets (Magnúsdóttir et al., 2013).

(E) Number of AKT targets in regulated modules of ESCs (Kim et al., 2010).

(F) The number of colonies at day 10 of the culture (top) and alkaline phosphatase (ALP) staining (bottom) are shown. Scale bar represents 7 mm (top). E11.5 PGCs were collected from AKT-Mer embryos based on SSEA-1 expression and induced to undergo conversion into EGCs by culture in ESC medium containing the specified chemicals. Data represent the mean \pm SD of independent experiments. Statistical significance was determined using Tukey's multiple comparison test ($n = 3$). ** $p < 0.01$.

(G) (Left) Typical morphology of ESC-like colonies derived from AKT-Mer PGCs at day 8. SSEA-1-positive PGCs were cultured in N2B27 medium containing bFGF, 4OHT, and 2i or 2i+A83 without feeder cells or serum replacement (KSR). The lower panels are higher magnification images of the upper panels. Scale bars represent 250 μ m (top) and 100 μ m (bottom). (Right) The number of colonies at day 8. Data represent the mean \pm SD of independent experiments. Statistical significance was determined using Student's t test ($n = 4$). * $p = 0.088$.

essential signal for the generation of EGCs from PGCs (Durcova-Hills et al., 2006), AKT activation has been reported to be sufficient to induce EGCs (Kimura et al., 2008). To analyze the effect of AKT activation, we used PGCs from *Akt-mer* Tg mice (Kimura et al., 2008). In these mice, AKT is activated by adding 4OHT. We found that AKT activation

induced EGCs from PGCs in the absence of bFGF (Figure 6A). To analyze the AKT signal, we collected AKT target molecules in ESCs from a previous report (Yamano et al., 2010). When the expression profiles of AKT targets were applied to our time course gene expression data, the AKT targets were shown to be activated from day 1 of the culture



(Figure 6B). These results indicated that the AKT targets were activated during pluripotency acquisition. Next, we analyzed AKT and other target genes. In the BLIMP-1 modules, the AKT targets did not largely overlap (overlap was highest in the BLIMP-1 PRC module, at 11.11%) (Figure 6C). In addition, all BLIMP-1 targets shared few targets with AKT (Figure 6D). Moreover, all ESC modules shared a few common targets with AKT (Figure 6E), suggesting that the effect of AKT activation on the dedifferentiation of PGCs is independent of BLIMP-1 targets or ESC modules. On the other hand, AKT activation is known to enhance the formation of EGCs from PGCs in the presence of bFGF (Kimura et al., 2008). In addition, although AKT activation induced EGCs in the absence of bFGF in the present study, 2i+A83 treatment enhanced the efficiency of this process (Figure 6A). We speculated that AKT has additive or synergistic effects with bFGF and/or 2i+A83. Therefore, we analyzed the combinatorial effect of bFGF, 2i+A83, and AKT activation. We found that AKT activation strongly enhanced EGC formation in the presence of bFGF and 2i+A83 (Figure 6F). Thus, AKT activation, bFGF, and 2i+A83 have a synergistic effect on the acquisition of pluripotency in PGCs. This combination of signals allowed us to generate EGCs even in the absence of feeder cells, serum, and serum replacement (KSR) (Figure 6G).

AKT Enhances the Acquisition of Pluripotency by Suppressing Mbd3

To understand how AKT signaling enhanced the acquisition of pluripotency in PGCs, we performed a whole-transcriptome analysis of cells subjected to each combination of treatments (Figure 7A). Inactivation of *Mbd3* was recently reported to greatly enhance the efficiency of reprogramming (Rais et al., 2013). This previous study identified the target genes of MBD3 by ChIP sequencing in untreated mouse embryonic fibroblasts (MEFs) and those transduced with four reprogramming factors (*Oct3/4*, *Sox2*, *Klf4*, and *c-Myc*, hereafter referred to as OSKM). We analyzed the expression profiles of these MBD3 target genes in the microarray data (Figure 7B). The heatmap results clearly showed that AKT signaling suppressed the MBD3 targets of OSKM-transduced MEFs. This tendency was also observed for the MBD3 targets of untreated MEFs (Figures S3A–S3D). To understand the function of the MBD3 targets of OSKM-transduced MEFs in PGCs, we analyzed the overlap between MBD3 targets and BLIMP-1 target genes. MBD3 targets in OSKM-transduced MEFs shared few targets with the BLIMP-1 modules or with all BLIMP-1 targets (Figures 7C and 7D). In addition, the ESC modules did not overlap with the MBD3 targets of OSKM-transduced MEFs (Figure 7E). Moreover, when looking at the microarray data of PGCs subjected to various treatments, we found that AKT activation was not corre-

lated with the changes in BLIMP-1 modules that accompanied EGC generation, namely, activation of the Core and Myc modules and suppression of the PRC module (Figure 7F). Taken together, these findings showed that AKT activation suppressed the MBD3 targets of OSKM-transduced MEFs in PGCs, which were different from the downstream targets of the BLIMP-1 and ESC modules. Finally, we analyzed whether AKT activation also downregulates MBD3 during somatic cell reprogramming. We found that, following the activation of AKT, MBD3 expression was suppressed in MEFs (Figures 7F and S3E). Furthermore, AKT activation at the early phase of somatic cell reprogramming enhanced the efficiency of this process (Figure 7H). Therefore, AKT activation enhanced pluripotency acquisition in MEFs via the suppression of MBD3-regulated genes.

DISCUSSION

We have identified that *Blimp-1* functions as a gatekeeper of pluripotency in PGCs. *Blimp-1* was originally identified as a transcriptional repressor in B cell maturation (Turner et al., 1994). During PGC specification, BLIMP-1 is important for the suppression of somatic cell programming (Kurimoto et al., 2008). The targets of BLIMP-1 may differ according to the situation. Transcription factors change the targets in a cell state-dependent manner. For example, Niwa et al. reported that the targets of SOX2 differed between ESCs and trophoblast stem cells because of different binding partners (Adachi et al., 2013). It is reported that BLIMP-1 binds the histone deacetylases TLE1 and EHMT2 in a context-dependent manner (Bikoff et al., 2009). It would be interesting to analyze the binding partners of BLIMP-1 during the specification of PGCs and induction of EGCs.

Whereas we found that *Blimp-1* deletion induced pluripotency in PGCs, the effects of *Blimp-1* overexpression in pluripotent cells appear to be more complicated. Forced expression of *Blimp-1* in ESCs induces growth retardation (Nagamatsu et al., 2011). During PGC induction from ESCs, induction of an intermediate cell state, namely epiblast-like cells (EpiLCs), is important (Hayashi et al., 2011). The combination of transcription factors *Prdm14*, *Blimp-1*, and *Tfap2c* is critical to induce PGCs from EpiLCs (Nakaki et al., 2013). However, forced induction of these three factors cannot induce PGCs directly from ESCs. Furthermore, whereas *Prdm14* alone can induce PGCs with low efficiency, *Blimp-1* alone cannot even induce PGCs from EpiLCs. Overexpression of *Prdm14* in ESCs enhances pluripotency maintenance but does not induce PGC differentiation (Okashita et al., 2014). These facts reveal that there are important differences between ESCs and EpiLCs in relation to PGC induction. One such

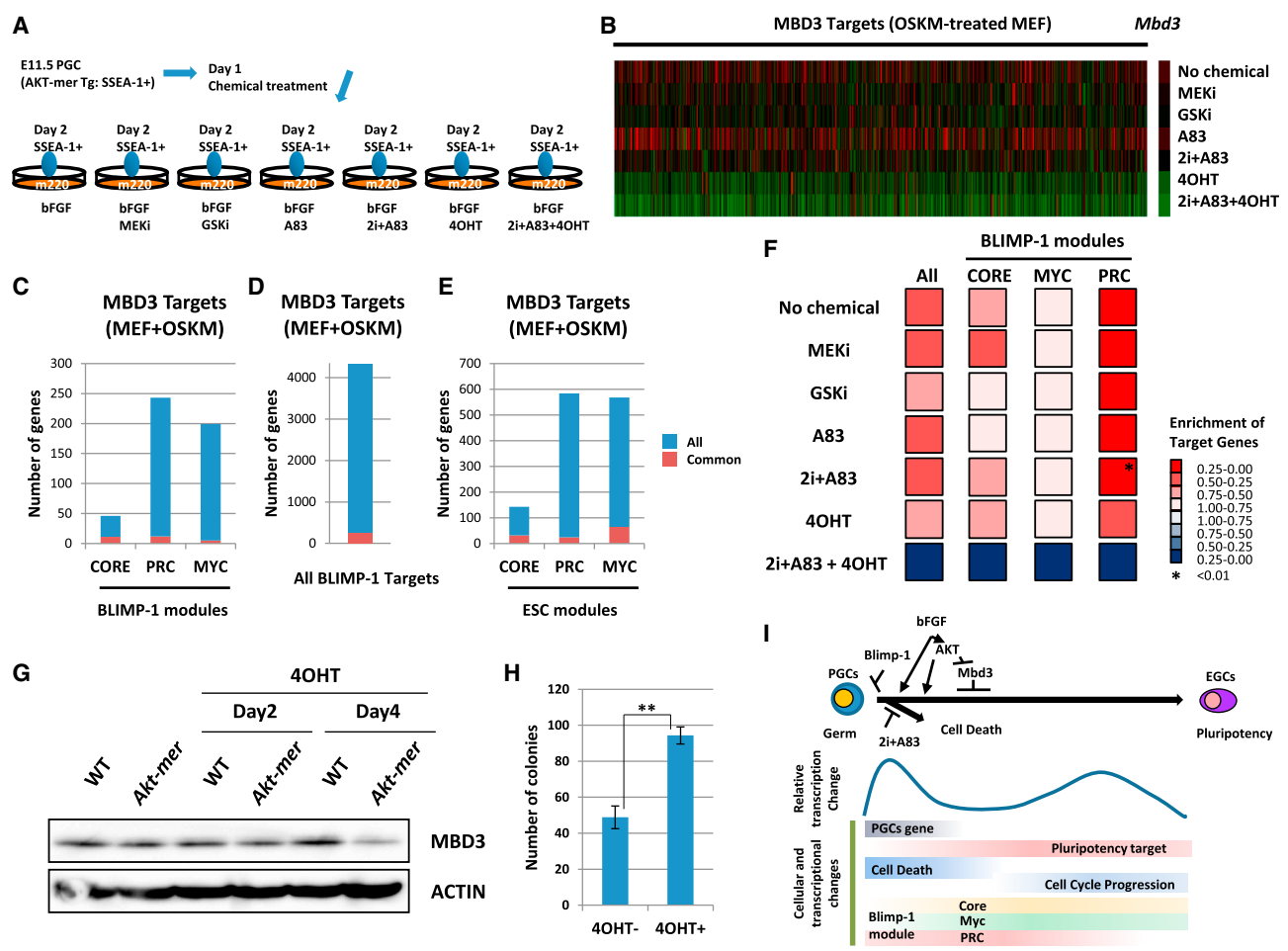


Figure 7. AKT Activation Suppresses Mbd3

(A–F) Summary of the procedure used to culture cells and isolate samples for microarray analysis (B–F). Gonads were surgically isolated from E11.5 AKT-mer embryos. After making a single cell suspension, PGCs were isolated based on SSEA-1 expression using a FACS AriaII cell sorter. Purified PGCs were seeded onto m220 feeder cells in ESC medium containing bFGF. One day after seeding, the indicated chemicals were added. On day 2, pluripotent candidate cells were sorted based on SSEA-1 expression for microarray analysis (Nagamatsu and Suda, 2013). 2i comprised inhibitors of MEK and glycogen synthase kinase- β (GSK3- β). A83 indicates the transforming growth factor- β (TGF- β) type 1R inhibitor. (B) Array heatmap analysis for pluripotent candidate cells at day 2 of each treatment. Mbd3 and Mbd3 targets of MEFs in which four reprogramming factors (*Oct3/4*, *Sox2*, *Klf4*, and *c-Myc* [OSKM]) were transduced are shown. These target genes are from Rais et al. (2013). (C) The number of MBD3 targets of OSKM-transduced MEFs in BLIMP-1 modules. Bars indicate the total number of genes in each BLIMP-1 module (Figure 4A). Red indicates MBD3 target genes of OSKM-transduced MEFs. (D) Number of MBD3 targets of OSKM-transduced MEFs among all BLIMP-1 targets (Magnúsdóttir et al., 2013). (E) Number of MBD3 targets of OSKM-transduced MEFs in ESC module (Kim et al., 2010). Bars indicate the total number of genes in each regulated module of ESCs. Red indicates MBD3 target genes of OSKM-transduced MEFs. (F) GSEA of BLIMP-1 targets for pluripotent candidate cells at day 2 of each treatment. BLIMP-1 modules were the gene sets identified in Figure 4.

(G) Western blotting of MBD3 after 4-hydroxytamoxifen (4OHT) treatment of MEFs isolated from WT and *Akt-mer* embryos. MEFs were treated with 4OHT (100 nM). At the indicated time points, MEFs were harvested and MBD3 expression was analyzed by western blot.

(H) The number of 3F (*Oct3/4*, *Sox2* and *Klf4*)-induced ESC-like colonies formed from *Akt-mer* MEFs, with or without 4OHT treatment at day 22. 4OHT was added at day 2 and allowed to react until day 6 after the 3F induction. Data represent the mean \pm SD of independent experiments. Statistical significance was determined using Student's t test ($n = 6$). ** $p < 0.01$.

(I) Gene expression regulation of cellular dynamics in the process of the acquisition of pluripotency in PGCs. Events identified in both the current study and a previous study (Nagamatsu et al., 2012a) are shown. The efficient dedifferentiation of *Mbd3* deficient PGCs was previously reported (Rais et al., 2013).

See also Figure S3.



difference is the existence of a suppressive mechanism in ESCs. Recently, it was reported that inactivation of *Myc* induces upregulation of germ cell marker genes in ESCs (Maeda et al., 2013). This indicates that PGC induction is suppressed in ESCs. However, in that report, *Vasa* was expressed much earlier than in vivo, and early markers, such as *Blimp-1*, were not activated efficiently. Therefore, it is unclear whether *Myc* inactivation induces functional differentiation. It would be intriguing to analyze differences between ESCs and EpiLCs in relation to the prerequisites for PGC differentiation.

To our surprise, overexpression of *Dnd* enhanced downstream targets of pluripotency (Figure 3). When *Dnd* is inactivated, the number of PGCs is decreased but basal PGCs give rise to teratomas in vivo (Youngren et al., 2005). Teratomas contain three germ layers generated by pluripotent cells. Therefore, deletion of *Dnd* leads to pluripotency in PGCs. However, in the present work, *Dnd* did not appear to mediate the suppression of pluripotency in ESCs. *Dnd* is not a target gene of either BLIMP-1 or AKT (Dataset S1), indicating that *Dnd* is regulated differently from BLIMP-1 or AKT. The mechanisms underlying pluripotency acquisition upon *Dnd* deletion, and the relationship between *Dnd* and *Blimp-1* or *Akt* in PGCs is an important issue to be investigated.

In this study, we found a synergistic effect of AKT activation in the presence of bFGF and 2i+A83 on the acquisition of pluripotency. AKT activation suppressed MBD3-regulated genes in PGCs (Figure 7B). Furthermore, AKT activation downregulated MBD3 in MEFs (Figure 7G). Both AKT activation and MBD3 inactivation have been shown to prevent differentiation of ESCs in the absence of LIF (Watanabe et al., 2006; Kaji et al., 2006). It is conceivable that AKT downregulates MBD3 and thereby maintains pluripotency in the absence of LIF. *Mbd3* is a roadblock of pluripotency (Rais et al., 2013). However, the regulation of *Mbd3* expression is poorly understood. It would be interesting to analyze how AKT signaling downregulates *Mbd3*.

It has been reported that a histone deacetylase (HDAC) inhibitor had a positive effect on EGC formation. We therefore analyzed AKT activation and HDAC target genes. For this purpose, we determined the genes that were upregulated in *Hdac*-deficient ESCs (Jamaladdin et al., 2014). GSEA analysis was performed at day 2 of the culture with or without AKT activation (Figure S3F). Whereas bFGF alone activated HDAC target genes, AKT activation suppressed this gene set, indicating that AKT enhances the formation of EGCs in a manner distinct from that of the HDAC pathway.

In this study, we used target gene set analysis. We considered that this approach would allow us to understand the gene network and epigenetic state, which are difficult to analyze based on the individual gene expressions. Whereas

both PGCs and EGCs express *Oct3/4*, the downstream targets of OCT3/4 were repressed from days 1 to 10 (Figures 2 and S1A). This indicated that the region downstream of OCT3/4 might differ between PGCs and EGCs. It was previously shown that *Oct3/4* plays a critical role in PGC specification (Okamura et al., 2008). It would thus be of interest to investigate the molecular interaction between *Oct3/4* and the factors that are important for PGC specification, such as *Blimp-1* and *Prdm14*. We also applied this approach to epigenetic modifications. First, we analyzed the histone modification-associated active genes (H3K36me3, H3K79me2, and H3K4me3) (Marson et al., 2008; Mikkelsen et al., 2007). The targets of these modifications were also gradually upregulated (Figure S1B). On the other hand, another set of modification targets consisting of H3K4me3, H3K27me3, or both (i.e., the Bivalent domain targets) showed intriguing change (Figure S1C). Whereas the targets of the Bivalent domain were upregulated in EGCs compared with early culture periods, the H3K27me3 targets were repressed. The targets of H3K4me3 were maintained in an active state. With respect to the targets of DNA methylation, three different gene sets of 5hmC and two different gene sets of 5meC were collected from three different papers (Pastor et al., 2011; Borgel et al., 2010; Guibert et al., 2012). Except for one time point (EGCs of Figure S1E), both the 5hmC and 5mC targets were activated from the early phase of the culture (Figures S1D–S1F). PGCs contain DNA with a low level of methylation (Seki et al., 2005). Therefore, it is feasible that the targets of DNA methylation in ESCs are already hypomethylated in PGCs and so easy for the early activation.

To understand how pluripotency is achieved, we compared somatic cell reprogramming with the acquisition of pluripotency in PGCs. Although these two phenomena are different, the obtained pluripotent stem cells have similar characteristics. Analysis of how pluripotent stem cells are generated from different cell types might help to clarify the mechanism of reprogramming. Of note, PGCs already have many similarities with pluripotent stem cells. Both processes showed two distinct waves of gene expression changes, in the early and late phases (Polo et al., 2012). During somatic cell reprogramming, both waves showed similar patterns of upregulated and downregulated genes. In contrast, during the acquisition of pluripotency in PGCs, the first and second waves were mainly composed of upregulated and downregulated genes, respectively (Figure 1E). These oppositely regulated genes are associated with the GO terms cell cycle, development, and metabolism (Table S1). In the early phase of somatic cell reprogramming, genes associated with “gain of proliferation”, “transient activation of developmental regulators”, and “metabolic changes” are regulated (Polo et al., 2012). Genes that are oppositely regulated during



the conversion of PGCs to EGCs might have an important role in somatic cell reprogramming. Furthermore, in both cases, cells lost their original characteristics during the early phase, after which genes in the pluripotency-associated network were upregulated. Comparison of these two types of pluripotency induction would improve our understanding of the reprogramming mechanisms and characteristics of PGCs. Taken together with the results of our previous study (Nagamatsu et al., 2012a), these findings summarize the process of acquisition of pluripotency in PGCs (Figure 7I).

This study presents precise information on gene expression profiles during the acquisition of pluripotency in PGCs. This information, in turn, provides mechanistic insights into the difference between PGCs and pluripotent stem cells and can be used to investigate the mechanism underlying somatic cell reprogramming. In future studies, it would be useful to compare distinct cell types and mechanisms to better understand the germ cell characteristics and reprogramming machinery.

EXPERIMENTAL PROCEDURES

Isolation and Culture of PGCs

PGCs were purified and cultured as described previously (Nagamatsu and Suda, 2013), and the detail is described in the Supplemental Information.

Microarray Analysis

Microarray analysis was performed using Whole Mouse Genome Oligo Microarray 44K (Agilent Technologies), and the detailed information is described in the Supplemental Information.

Generation and Isolation of ESCs Expressing Germ Cell Genes

Germ cell factors were introduced into EBRTcH3 ESCs as described in a previous report (Masui et al., 2005), and the detail is described in the Supplemental Information.

Teratoma Formation and Alkaline Phosphatase Staining

Teratoma formation and alkaline phosphatase staining were performed as described previously (Nagamatsu et al., 2012a), and the detail is described in the Supplemental Information.

Antibodies

The monoclonal antibodies used for western blotting were rabbit anti-MBD3 (ab157464; Abcam) and rabbit anti- β -ACTIN (A-2066; Sigma).

iPSC Generation

AKT-mer MEFs were reprogrammed using *Oct3/4*, *Sox2*, and *Klf4* as described previously (Nagamatsu et al., 2012b). 4OHT was added at day 2 and allowed to react to day 6 after the three-factor induction.

The numbers of morphologically ESC-like colonies were counted at day 22.

ACCESSION NUMBERS

The accession number of the microarray data in this study is GEO: GSE67616.

SUPPLEMENTAL INFORMATION

Supplemental Information includes Supplemental Experimental Procedures, three figures, two tables, and one dataset and can be found with this article online at <http://dx.doi.org/10.1016/j.stemcr.2015.05.007>.

AUTHOR CONTRIBUTIONS

G.N., K.T., and T.S. designed the project. G.N. performed the experiments and generated the figures. S.S. performed bioinformatics analysis, and G.N. and T.S. wrote the manuscript.

ACKNOWLEDGMENTS

We thank Dr. A. Tarakhovskiy (Rockefeller University) for providing the *Blimp-1^{flox/flox}* mice and Dr. T. Nakano and Dr. T. Kimura (Osaka University) for providing the AKT-Mer mice. We also thank Dr. K. Hosokawa (Kyushu University) for providing the recombinant CRE protein and Dr. K. Hayashi (Kyushu University) for a critical reading of this manuscript. This study was supported in part by a grant from the Project for Realization of Regenerative Medicine. Support for the Core Institutes for iPS Cell Research was provided by MEXT and the Keio University Medical Science Fund. G.N. was supported by a PRESTO grant of the Japan Science and Technology Agency and by Funds for the Development of Human Resources in Science and Technology of the Program to Disseminate a Tenure Tracking System for the Tenure-Track Program at the Sakauchi Laboratory.

Received: November 3, 2014

Revised: May 7, 2015

Accepted: May 7, 2015

Published: June 4, 2015

REFERENCES

- Adachi, K., Nikaido, I., Ohta, H., Ohtsuka, S., Ura, H., Kadota, M., Wakayama, T., Ueda, H.R., and Niwa, H. (2013). Context-dependent wiring of Sox2 regulatory networks for self-renewal of embryonic and trophoblast stem cells. *Mol. Cell* 52, 380–392.
- Bikoff, E.K., Morgan, M.A., and Robertson, E.J. (2009). An expanding job description for *Blimp-1/PRDM1*. *Curr. Opin. Genet. Dev.* 19, 379–385.
- Borgel, J., Guibert, S., Li, Y., Chiba, H., Schübeler, D., Sasaki, H., Forné, T., and Weber, M. (2010). Targets and dynamics of promoter DNA methylation during early mouse development. *Nat. Genet.* 42, 1093–1100.
- Durcova-Hills, G., Adams, I.R., Barton, S.C., Surani, M.A., and McLaren, A. (2006). The role of exogenous fibroblast growth



- factor-2 on the reprogramming of primordial germ cells into pluripotent stem cells. *Stem Cells* 24, 1441–1449.
- Guibert, S., Forné, T., and Weber, M. (2012). Global profiling of DNA methylation erasure in mouse primordial germ cells. *Genome Res.* 22, 633–641.
- Hayashi, K., Ohta, H., Kurimoto, K., Aramaki, S., and Saitou, M. (2011). Reconstitution of the mouse germ cell specification pathway in culture by pluripotent stem cells. *Cell* 146, 519–532.
- Hu, G., and Wade, P.A. (2012). NuRD and pluripotency: a complex balancing act. *Cell Stem Cell* 10, 497–503.
- Jamaladdin, S., Kelly, R.D., O'Regan, L., Dovey, O.M., Hodson, G.E., Millard, C.J., Portolano, N., Fry, A.M., Schwabe, J.W., and Cowley, S.M. (2014). Histone deacetylase (HDAC) 1 and 2 are essential for accurate cell division and the pluripotency of embryonic stem cells. *Proc. Natl. Acad. Sci. USA* 111, 9840–9845.
- Jeong, H., Mason, S.P., Barabási, A.L., and Oltvai, Z.N. (2001). Lethality and centrality in protein networks. *Nature* 411, 41–42.
- Kaji, K., Caballero, I.M., MacLeod, R., Nichols, J., Wilson, V.A., and Hendrich, B. (2006). The NuRD component Mbd3 is required for pluripotency of embryonic stem cells. *Nat. Cell Biol.* 8, 285–292.
- Kim, J., Chu, J., Shen, X., Wang, J., and Orkin, S.H. (2008). An extended transcriptional network for pluripotency of embryonic stem cells. *Cell* 132, 1049–1061.
- Kim, J., Woo, A.J., Chu, J., Snow, J.W., Fujiwara, Y., Kim, C.G., Cantor, A.B., and Orkin, S.H. (2010). A Myc network accounts for similarities between embryonic stem and cancer cell transcription programs. *Cell* 143, 313–324.
- Kimura, T., Tomooka, M., Yamano, N., Murayama, K., Matoba, S., Umehara, H., Kanai, Y., and Nakano, T. (2008). AKT signaling promotes derivation of embryonic germ cells from primordial germ cells. *Development* 135, 869–879.
- Kurimoto, K., Yabuta, Y., Ohinata, Y., Shigeta, M., Yamanaka, K., and Saitou, M. (2008). Complex genome-wide transcription dynamics orchestrated by Blimp1 for the specification of the germ cell lineage in mice. *Genes Dev.* 22, 1617–1635.
- Leitch, H.G., Blair, K., Mansfield, W., Ayetey, H., Humphreys, P., Nichols, J., Surani, M.A., and Smith, A. (2010). Embryonic germ cells from mice and rats exhibit properties consistent with a generic pluripotent ground state. *Development* 137, 2279–2287.
- Leitch, H.G., Okamura, D., Durcova-Hills, G., Stewart, C.L., Gardner, R.L., Matsui, Y., and Papaioannou, V.E. (2014). On the fate of primordial germ cells injected into early mouse embryos. *Dev. Biol.* 385, 155–159.
- Maeda, I., Okamura, D., Tokitake, Y., Ikeda, M., Kawaguchi, H., Mise, N., Abe, K., Noce, T., Okuda, A., and Matsui, Y. (2013). Max is a repressor of germ cell-related gene expression in mouse embryonic stem cells. *Nat. Commun.* 4, 1754.
- Magnúsdóttir, E., Dietmann, S., Murakami, K., Günesdogan, U., Tang, F., Bao, S., Diamanti, E., Lao, K., Gottgens, B., and Azim Surani, M. (2013). A tripartite transcription factor network regulates primordial germ cell specification in mice. *Nat. Cell Biol.* 15, 905–915.
- Marson, A., Levine, S.S., Cole, M.F., Frampton, G.M., Brambrink, T., Johnstone, S., Guenther, M.G., Johnston, W.K., Wernig, M., Newman, J., et al. (2008). Connecting microRNA genes to the core transcriptional regulatory circuitry of embryonic stem cells. *Cell* 134, 521–533.
- Masui, S., Shimosato, D., Toyooka, Y., Yagi, R., Takahashi, K., and Niwa, H. (2005). An efficient system to establish multiple embryonic stem cell lines carrying an inducible expression unit. *Nucleic Acids Res.* 33, e43.
- Matsui, Y., Zsebo, K., and Hogan, B.L. (1992). Derivation of pluripotent embryonic stem cells from murine primordial germ cells in culture. *Cell* 70, 841–847.
- Mikkelsen, T.S., Ku, M., Jaffe, D.B., Issac, B., Lieberman, E., Gianoukos, G., Alvarez, P., Brockman, W., Kim, T.K., Koche, R.P., et al. (2007). Genome-wide maps of chromatin state in pluripotent and lineage-committed cells. *Nature* 448, 553–560.
- Nagamatsu, G., and Suda, T. (2013). Conversion of primordial germ cells to pluripotent stem cells: methods for cell tracking and culture conditions. *Methods Mol. Biol.* 1052, 49–56.
- Nagamatsu, G., Kosaka, T., Kawasumi, M., Kinoshita, T., Takubo, K., Akiyama, H., Sudo, T., Kobayashi, T., Oya, M., and Suda, T. (2011). A germ cell-specific gene, Prmt5, works in somatic cell reprogramming. *J. Biol. Chem.* 286, 10641–10648.
- Nagamatsu, G., Kosaka, T., Saito, S., Takubo, K., Akiyama, H., Sudo, T., Horimoto, K., Oya, M., and Suda, T. (2012a). Tracing the conversion process from primordial germ cells to pluripotent stem cells in mice. *Biol. Reprod.* 86, 182.
- Nagamatsu, G., Saito, S., Kosaka, T., Takubo, K., Kinoshita, T., Oya, M., Horimoto, K., and Suda, T. (2012b). Optimal ratio of transcription factors for somatic cell reprogramming. *J. Biol. Chem.* 287, 36273–36282.
- Nagamatsu, G., Kosaka, T., Saito, S., Honda, H., Takubo, K., Kinoshita, T., Akiyama, H., Sudo, T., Horimoto, K., Oya, M., and Suda, T. (2013). Induction of pluripotent stem cells from primordial germ cells by single reprogramming factors. *Stem Cells* 31, 479–487.
- Nakaki, F., Hayashi, K., Ohta, H., Kurimoto, K., Yabuta, Y., and Saitou, M. (2013). Induction of mouse germ-cell fate by transcription factors in vitro. *Nature* 501, 222–226.
- Ohinata, Y., Payer, B., O'Carroll, D., Ancelin, K., Ono, Y., Sano, M., Barton, S.C., Obukhanych, T., Nussenzweig, M., Tarakhovskiy, A., et al. (2005). Blimp1 is a critical determinant of the germ cell lineage in mice. *Nature* 436, 207–213.
- Okamura, D., Tokitake, Y., Niwa, H., and Matsui, Y. (2008). Requirement of Oct3/4 function for germ cell specification. *Dev. Biol.* 317, 576–584.
- Okashita, N., Kumaki, Y., Ebi, K., Nishi, M., Okamoto, Y., Nakayama, M., Hashimoto, S., Nakamura, T., Sugawara, K., Kojima, N., et al. (2014). PRDM14 promotes active DNA demethylation through the ten-eleven translocation (TET)-mediated base excision repair pathway in embryonic stem cells. *Development* 141, 269–280.
- Pastor, W.A., Pape, U.J., Huang, Y., Henderson, H.R., Lister, R., Ko, M., McLoughlin, E.M., Brudno, Y., Mahapatra, S., Kapranov, P., et al. (2011). Genome-wide mapping of 5-hydroxymethylcytosine in embryonic stem cells. *Nature* 473, 394–397.
- Polo, J.M., Anderssen, E., Walsh, R.M., Schwarz, B.A., Nefzger, C.M., Lim, S.M., Borkent, M., Apostolou, E., Alaei, S., Cloutier, J.,



- et al. (2012). A molecular roadmap of reprogramming somatic cells into iPS cells. *Cell* 151, 1617–1632.
- Rais, Y., Zviran, A., Geula, S., Gafni, O., Chomsky, E., Viukov, S., Mansour, A.A., Caspi, I., Krupalnik, V., Zerbib, M., et al. (2013). Deterministic direct reprogramming of somatic cells to pluripotency. *Nature* 502, 65–70.
- Saitou, M., and Yamaji, M. (2012). Primordial germ cells in mice. *Cold Spring Harb. Perspect. Biol.* 4, a008375.
- Sasaki, H., and Matsui, Y. (2008). Epigenetic events in mammalian germ-cell development: reprogramming and beyond. *Nat. Rev. Genet.* 9, 129–140.
- Seki, Y., Hayashi, K., Itoh, K., Mizugaki, M., Saitou, M., and Matsui, Y. (2005). Extensive and orderly reprogramming of genome-wide chromatin modifications associated with specification and early development of germ cells in mice. *Dev. Biol.* 278, 440–458.
- Suzuki, A., Tsuda, M., and Saga, Y. (2007). Functional redundancy among Nanos proteins and a distinct role of Nanos2 during male germ cell development. *Development* 134, 77–83.
- Suzuki, H., Tsuda, M., Kiso, M., and Saga, Y. (2008). Nanos3 maintains the germ cell lineage in the mouse by suppressing both Bax-dependent and -independent apoptotic pathways. *Dev. Biol.* 318, 133–142.
- Takahashi, K., and Yamanaka, S. (2006). Induction of pluripotent stem cells from mouse embryonic and adult fibroblast cultures by defined factors. *Cell* 126, 663–676.
- Tanaka, S.S., Toyooka, Y., Akasu, R., Katoh-Fukui, Y., Nakahara, Y., Suzuki, R., Yokoyama, M., and Noce, T. (2000). The mouse homolog of *Drosophila Vasa* is required for the development of male germ cells. *Genes Dev.* 14, 841–853.
- Turner, C.A., Jr., Mack, D.H., and Davis, M.M. (1994). Blimp-1, a novel zinc finger-containing protein that can drive the maturation of B lymphocytes into immunoglobulin-secreting cells. *Cell* 77, 297–306.
- Watanabe, S., Umehara, H., Murayama, K., Okabe, M., Kimura, T., and Nakano, T. (2006). Activation of Akt signaling is sufficient to maintain pluripotency in mouse and primate embryonic stem cells. *Oncogene* 25, 2697–2707.
- Weber, S., Eckert, D., Nettersheim, D., Gillis, A.J., Schäfer, S., Kuckenberger, P., Ehlermann, J., Werling, U., Biermann, K., Looijenga, L.H., and Schorle, H. (2010). Critical function of AP-2 gamma/TCFAP2C in mouse embryonic germ cell maintenance. *Biol. Reprod.* 82, 214–223.
- Yamaji, M., Seki, Y., Kurimoto, K., Yabuta, Y., Yuasa, M., Shigeta, M., Yamanaka, K., Ohinata, Y., and Saitou, M. (2008). Critical function of Prdm14 for the establishment of the germ cell lineage in mice. *Nat. Genet.* 40, 1016–1022.
- Yamaji, M., Ueda, J., Hayashi, K., Ohta, H., Yabuta, Y., Kurimoto, K., Nakato, R., Yamada, Y., Shirahige, K., and Saitou, M. (2013). PRDM14 ensures naive pluripotency through dual regulation of signaling and epigenetic pathways in mouse embryonic stem cells. *Cell Stem Cell* 12, 368–382.
- Yamano, N., Kimura, T., Watanabe-Kushima, S., Shinohara, T., and Nakano, T. (2010). Metastable primordial germ cell-like state induced from mouse embryonic stem cells by Akt activation. *Biochem. Biophys. Res. Commun.* 392, 311–316.
- Ying, Q.L., Wray, J., Nichols, J., Batlle-Morera, L., Doble, B., Woodgett, J., Cohen, P., and Smith, A. (2008). The ground state of embryonic stem cell self-renewal. *Nature* 453, 519–523.
- Youngren, K.K., Coveney, D., Peng, X., Bhattacharya, C., Schmidt, L.S., Nickerson, M.L., Lamb, B.T., Deng, J.M., Behringer, R.R., Capel, B., et al. (2005). The Ter mutation in the dead end gene causes germ cell loss and testicular germ cell tumours. *Nature* 435, 360–364.
- Yuan, X., Wan, H., Zhao, X., Zhu, S., Zhou, Q., and Ding, S. (2011). Brief report: combined chemical treatment enables Oct4-induced reprogramming from mouse embryonic fibroblasts. *Stem Cells* 29, 549–553.

Stem Cell Reports

Supplemental Information

**Integrative Analysis of the Acquisition
of Pluripotency in PGCs Reveals the Mutually
Exclusive Roles of Blimp-1 and AKT Signaling**

Go Nagamatsu, Shigeru Saito, Keiyo Takubo, and Toshio Suda

Supplemental experimental procedures

Mice

Blimp-1^{flox/flox} mice were the kind gift of Dr. A. Tarakhovsky (Rockefeller University)(Ohinata et al., 2005). *Akt-mer* transgenic mice were the kind gift of Drs. T. Kimura and T. Nakano (Osaka University)(Kimura et al., 2008). *Akt-mer* transgenic mice were crossed with ICR for more than 6 generations. ICR and Balb/c nude mice were purchased from Japan SLC (Shizuoka, Japan). Animal care was performed in accordance with the guidelines established by Keio University for animal use and recombinant DNA experiments.

Isolation and culture of PGCs

PGCs were purified by SSEA-1 staining and using a BD FACS AriaII cell sorter (BD Bioscience). Sorted PGCs were cultured on Sl/Sl⁴-m220 or STO feeder cells in Knockout DMEM (Invitrogen) supplemented with 15% KSR (Invitrogen), 2 mM glutamine, 1 mM non-essential amino acids, 2- β -mercaptoethanol, LIF, and bFGF. The chemical compounds used in this study were PD325901 (1 μ M), CHIR99021 (3 μ M), and A83-01 (250 nM), which respectively inhibit MEK, GSK3- β , and TGF- β R. At day 7 (on m220 cells) or day 6 (on STO cells), the bFGF-containing medium was replaced with fresh medium lacking bFGF. In the case of seeding on Sl/Sl⁴-m220 cells, cells were collected and reseeded onto STO feeder cells on day 3 of culture. For deletion of floxed Blimp-1 in PGCs, sorted PGCs were incubated with recombinant-Cre (the kind gift of Dr. K. Hosokawa) at 37°C for 30 min. After washing, the cells were seeded. In the case of AKT activation, 4-hydroxytamoxifen (Sigma) was added at a concentration of 100 nM. For the feeder cell-free method, the culture conditions were identical to those for the ESC

culture(Hayashi and Saitou, 2013).

Microarray analysis

Total RNA was extracted by RNeasy Plus Micro kit (Qiagen) according to manufacturers' manual. The quality of purified total RNA was verified by an Agilent 2100 bioanalyzer (Agilent technologies). Isolated total RNA was converted into cDNA. Cyanine-3 labeled cDNA was prepared using Genomic Enzymatic Labeling Kit (Agilent technologies) according to the manufacturer's instructions, followed by MinElute column purification. Labeled cDNA was hybridized to Whole Mouse Genome Oligo Microarray 44K (Agilent Technologies) for 17 hr at 65°C. The microarray was scanned by an Agilent Scanner, and the scan image data was analyzed with Feature Extraction software (Agilent Technologies). To perform gene-level interpretation, the whole probes were collapsed into genes with Entrez Gene ID by taking the maximum intensity among probe sets targeting the same gene. Differential gene expression analysis was performed using the fold-change method. Gene expression changes of >2-fold were considered significant. Heat maps were produced by color-coding with the Z scores of samples. To confirm the existence of genes that are gradually expressed during the acquisition of pluripotency, genes that showed expression changes at each time point were extracted. PCA and GO analysis were performed with these gradually expressed genes using the prcomp function of the R statistical package. To characterise the molecular backgrounds of the genes that were oppositely regulated during the two waves, an enrichment analysis of canonical pathways and GO biological processes on the generic GO slim subset was performed using the GO Term Finder(Boyle et al., 2004). Thereafter, the family-wise error rate (FWER) was estimated. The Gene Expression

Omnibus (GEO) database accession number of the microarray data in this study is GSE67616.

GSEA

GSEA was performed to determine whether the expression of downstream targets increased or decreased. GSEA was performed using GSEA version 2.0.10 from the Broad Institute according to the pre-ranked list protocol using the gene sets defined in the Dataset S1. The pre-ranked lists were calculated based on the fold-change in expression. The downstream expression status was judged using the crude nominal p value in the GSEA results.

Generation and isolation of ESCs expressing germ cell genes

Germ cell factors were cloned into the *pZhc* exchange vector. The exchange vectors and *pCAGGS-Cre* were transfected using Lipofectamine 2000 (Invitrogen) according to the manufacturer's instructions. Two days after transfection, ESCs were selected using Zeocin and resistant colonies were isolated. The established lines were treated with doxycycline, and GFP-positive cells were purified using a FACS AriaII cell sorter (BD Bioscience) for microarray analysis. In the case of *Blimp-1* overexpression, EBRTcH3 ESCs were transfected with *pEF1a-IRES-AcGFP* (TaKaRa) or *pEF1a-Blimp-1-IRES-AcGFP* using Lipofectamine 2000 according to the manufacturer's instructions. Two days after transfection, AcGFP-positive cells were purified using a FACS AriaII cell sorter (BD Bioscience) for microarray analysis.

Gene expression analysis

Transcript levels were determined using the 7500 Fast Real-Time PCR system (Applied Biosystems) with a Taqman assay mix (Applied Biosystems). The assay mix used for each genes were following: *Prdm14* (Mm01237813_m1), *Vasa* (Mm00802445_m1), *Nanos2* (Mm02525720_s1), *Nanos3* (Mm00808138_m1), *Dnd* (Mm00849348_s1), *Blimp-1* (Mm01187285_m1), *Klf4* (Mm00516104_m1) and *Eras* (Mm03053919_s1).

Genomic PCR analysis for Blimp-1 floxed and deletion alleles

Genotypes of *Blimp-1* flox and deletion were determined by genomic PCR using three primers: a forward primer for both floxed and deleted alleles (5'-GCCCAGTGACTCAAAGCACTA -3'), a reverse primer for the floxed allele (5'-TATGGTCTTCTCATGTTGGGG -3'), and a reverse primer for the deleted allele (5'-GGTGTCTGAAGAGCAAAGCTG -3'). Genomic PCR was performed under the following conditions: 35 cycles of 94°C for 30 s, 59°C for 30 s, and 72°C for 30 s.

Teratoma formation

Cells (1.0×10^6) were suspended in Matrigel (BD) and injected into nude mice. After 3–4 weeks, the tumours were fixed with 4% paraformaldehyde (PFA) prepared in phosphate-buffered saline (PBS), embedded in paraffin, sectioned, and stained with hematoxylin and eosin.

Alkaline phosphatase staining

ESCs were fixed at 4°C for 10 min with 4% PFA prepared in PBS, washed twice with PBS, and stained at 37°C for 30 min using the SCIP/NBT liquid substrate system (B-1911; Sigma).

Induction of EGCs from PGCLCs

Doxycycline-inducible *Blimp-1* ESCs that contained *Blimp-1-Venus* and *Stella-CFP* were the kind gift of Dr. M. Saitou (Kyoto University) (Nakaki et al., 2013). PGCLCs were induced from ESCs according to the method in a previous report (Hayashi et al., 2011). At day 6 of induction, PGCLCs were sorted by *Blimp-1-Venus* fluorescence. Sorted PGCLCs were cultured as EGCs induced from E11.5 PGCs. One day after EGC induction, doxycycline (1.5 µg/ml) was added to the culture at the indicated time periods. The numbers of ESC-like colonies were counted at day 10 after EGC induction.

Quantification of western blot analysis

Chemiluminescence intensity of western blot analysis was numerically converted by using FusionCapt Advance Solo 4 S (VILBER LOURMAT) software.

Supplementary Figure Legends

Supplementary Figure S1. a. Gene expression changes of core transcription factors in ESCs during the acquisition of pluripotency from PGCs. **b-f** Gene Set Enrichment Analysis (GSEA) of downstream targets of epigenetic modification. **b, c.** GSEA of downstream targets of histone modifications from Marson A et al.(Marson et al., 2008) (b) and Mikkelsen TS et al.(Mikkelsen et al., 2007) (c). **d-f.** GSEA of downstream targets of DNA methylation from Pastor WA et al.(Pastor et al., 2011) (d), Borgel J et al.(Borgel et al., 2010) (e) and Guibert S et al.(Guibert et al., 2012) (f). 5hmC represents 5-(Hydroxy)methylcytosine and 5meC represents 5-methylcytosine.

Supplementary Figure S2. a. Genomic PCR analysis of EGCs generated from PGCs that were treated with PBS and cultured in the presence of bFGF or treated with rCre and cultured in the absence of bFGF. The *Blimp-1* floxed allele (250 bp) and *Blimp-1* deletion allele (410 bp) are shown. **b.** Forced expression of *Blimp-1* during EGC formation from PGCLCs. The number of ESC-like colonies observed from PGCLCs at 10 days after EGCs induction. *Blimp-1* was induced by adding doxycycline at the indicated time points. Data represent the mean \pm SD of independent experiments. Statistical significance was determined using Tukey's multiple comparison test ($n = 4$ for no treatment, $n = 3$ for day1-3 on m220, $n = 4$ for day1-7),

Supplementary Figure S3. a. Array heat map analysis for pluripotent candidate cells at day 2 of each treatment. *Mbd3* and MBD3 targets of mouse embryonic fibroblasts (MEFs) are shown. These target genes are from Rais et al.(Rais et al., 2013). **b.** The number of MBD3 targets of MEFs in BLIMP-1 modules. Bars indicate the total number

of genes in each BLIMP-1 module (Figure 4a). Red indicates MBD3 target genes of MEFs. **c.** Number of MBD3 targets of MEFs among all BLIMP-1 targets (Magnusdottir et al., 2013). **d.** Number of MBD3 targets of MEFs in ESC module (Kim et al., 2010). Bars indicate the total number of genes in each regulated module of ESCs. Red indicates MBD3 target genes of MEFs. **e.** Quantification of MBD3 expression of western blot shown in Figure 7g. The MBD3 expression level was normalized by the ACTIN expression level. Relative expression level was shown as *Akt-mer* / WT at each day of the culture. Dots represent the numbers of each experiment and the bar indicates the median. Statistical significance was determined using a one-sided t-test (independent experiments, $n = 3$). #P=0.0512. **f.** GSEA of upregulated genes in *Hdac*-deficient ES cells from Jamaladdin S et al. (Jamaladdin et al., 2014).

Supplementary Table S2. Genes shared by more than 7 of 9 regulatory factors

	<u>Day 1</u>	<u>Day 2</u>	<u>Day 3</u>	<u>Day 6</u>	<u>Day 10</u>	<u>EGCs</u>
<i>Klf9</i>	*	*	*	*	*	*
<i>Tmem131</i>	*	*	*	*	*	*
<i>Dido1</i>	*	*		*	*	*
<i>Rarg</i>	*	*		*	*	*
<i>Trim8</i>	*	*		*	*	*
<i>Mybl2</i>	*			*	*	*
<i>Nid2</i>	*	*			*	*
<i>Nolc1</i>	*	*			*	*
<i>Zfp704</i>	*				*	*
<i>Trim25</i>	*					
<i>Chd9</i>		*			*	*
<i>Gpa33</i>				*	*	*
<i>Lrrc2</i>				*	*	*
<i>Tdgf1</i>				*	*	*
<i>Tgif1</i>				*	*	*
<i>Zscan10</i>				*	*	*
<i>Gm13051</i>					*	*
<i>Tcea3</i>					*	*
<i>Slc20a1</i>					*	*
<i>Asx11</i>						*
<i>Cbx7</i>						*
<i>E2F4</i>						*
<i>Gm13154</i>						*
<i>Gm13212</i>						*
<i>Msh6</i>						*
<i>Pou5f1</i>						*
<i>Rest</i>						*
<i>Rlim</i>						*
<i>Rmnd5b</i>						*
<i>Sfrp1</i>						*
<i>Sulf2</i>						*
<i>Zfp532</i>						*
<i>Zic2</i>						*

Zic5

*

2410137M14Rik

*

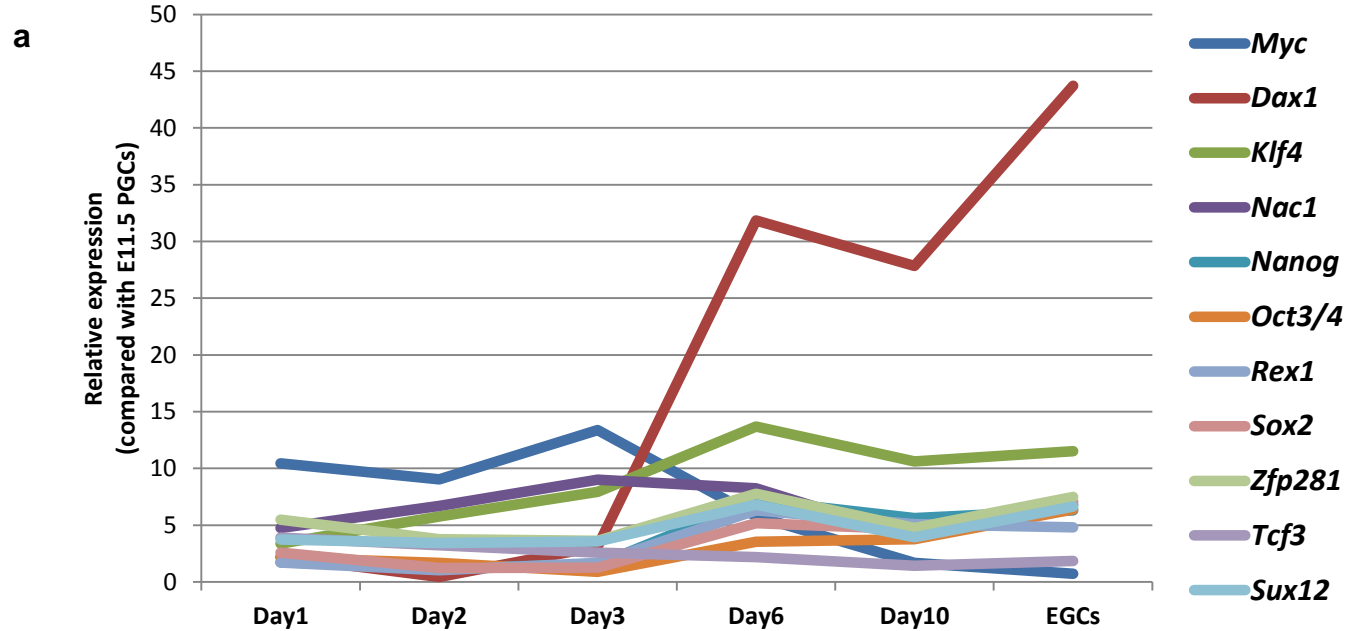
5730390G19Rik

*

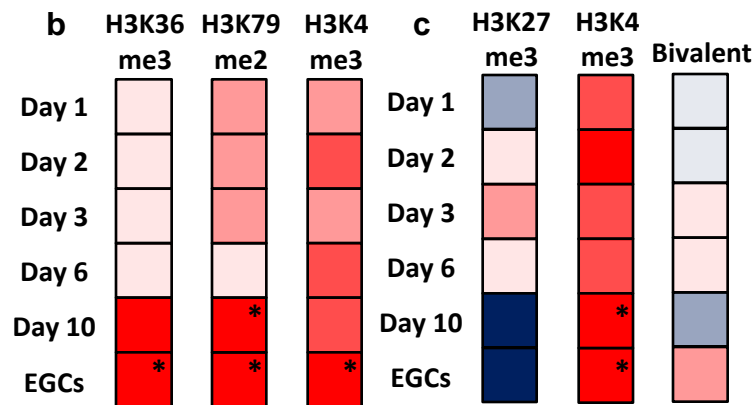
Supplementary References

- Borgel, J., Guibert, S., Li, Y., Chiba, H., Schubeler, D., Sasaki, H., Forne, T., and Weber, M. (2010). Targets and dynamics of promoter DNA methylation during early mouse development. *Nat Genet* *42*, 1093-1100.
- Boyle, E.I., Weng, S., Gollub, J., Jin, H., Botstein, D., Cherry, J.M., and Sherlock, G. (2004). GO::TermFinder--open source software for accessing Gene Ontology information and finding significantly enriched Gene Ontology terms associated with a list of genes. *Bioinformatics* *20*, 3710-3715.
- Guibert, S., Forne, T., and Weber, M. (2012). Global profiling of DNA methylation erasure in mouse primordial germ cells. *Genome Res* *22*, 633-641.
- Hayashi, K., Ohta, H., Kurimoto, K., Aramaki, S., and Saitou, M. (2011). Reconstitution of the mouse germ cell specification pathway in culture by pluripotent stem cells. *Cell* *146*, 519-532.
- Hayashi, K., and Saitou, M. (2013). Stepwise differentiation from naive state pluripotent stem cells to functional primordial germ cells through an epiblast-like state. *Methods Mol Biol*, 628-623_613.
- Jamaladdin, S., Kelly, R.D., O'Regan, L., Dovey, O.M., Hodson, G.E., Millard, C.J., Portolano, N., Fry, A.M., Schwabe, J.W., and Cowley, S.M. (2014). Histone deacetylase (HDAC) 1 and 2 are essential for accurate cell division and the pluripotency of embryonic stem cells. *Proc Natl Acad Sci U S A* *111*, 9840-9845.
- Kimura, T., Tomooka, M., Yamano, N., Murayama, K., Matoba, S., Umehara, H., Kanai, Y., and Nakano, T. (2008). AKT signaling promotes derivation of embryonic germ cells from primordial germ cells. *Development* *135*, 869-879.
- Marson, A., Levine, S.S., Cole, M.F., Frampton, G.M., Brambrink, T., Johnstone, S., Guenther, M.G., Johnston, W.K., Wernig, M., Newman, J., *et al.* (2008). Connecting microRNA genes to the core transcriptional regulatory circuitry of embryonic stem cells. *Cell* *134*, 521-533.
- Mikkelsen, T.S., Ku, M., Jaffe, D.B., Issac, B., Lieberman, E., Giannoukos, G., Alvarez, P., Brockman, W., Kim, T.K., Koche, R.P., *et al.* (2007). Genome-wide maps of chromatin state in pluripotent and lineage-committed cells. *Nature* *448*, 553-560.
- Nakaki, F., Hayashi, K., Ohta, H., Kurimoto, K., Yabuta, Y., and Saitou, M. (2013). Induction of mouse germ-cell fate by transcription factors in vitro. *Nature* *501*, 222-226.
- Ohinata, Y., Payer, B., O'Carroll, D., Ancelin, K., Ono, Y., Sano, M., Barton, S.C., Obukhanych, T., Nussenzweig, M., Tarakhovskiy, A., *et al.* (2005). Blimp1 is a critical determinant of the germ cell lineage in mice. *Nature* *436*, 207-213.
- Pastor, W.A., Pape, U.J., Huang, Y., Henderson, H.R., Lister, R., Ko, M., McLoughlin,

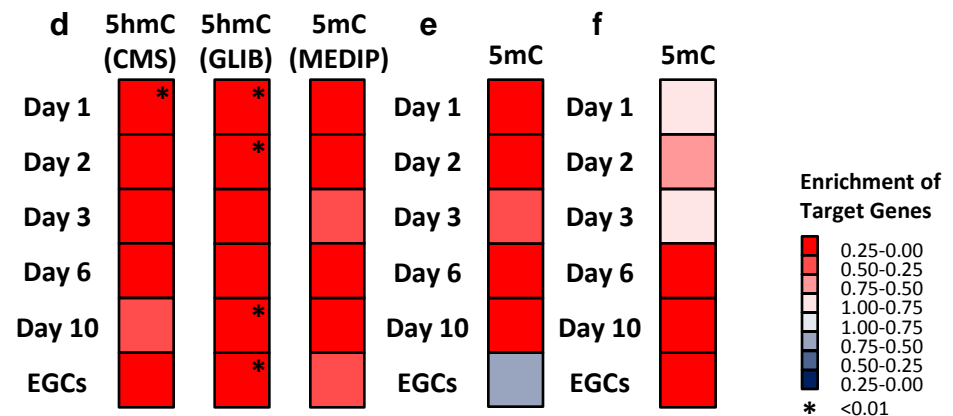
E.M., Brudno, Y., Mahapatra, S., Kapranov, P., *et al.* (2011). Genome-wide mapping of 5-hydroxymethylcytosine in embryonic stem cells. *Nature* 473, 394-397.

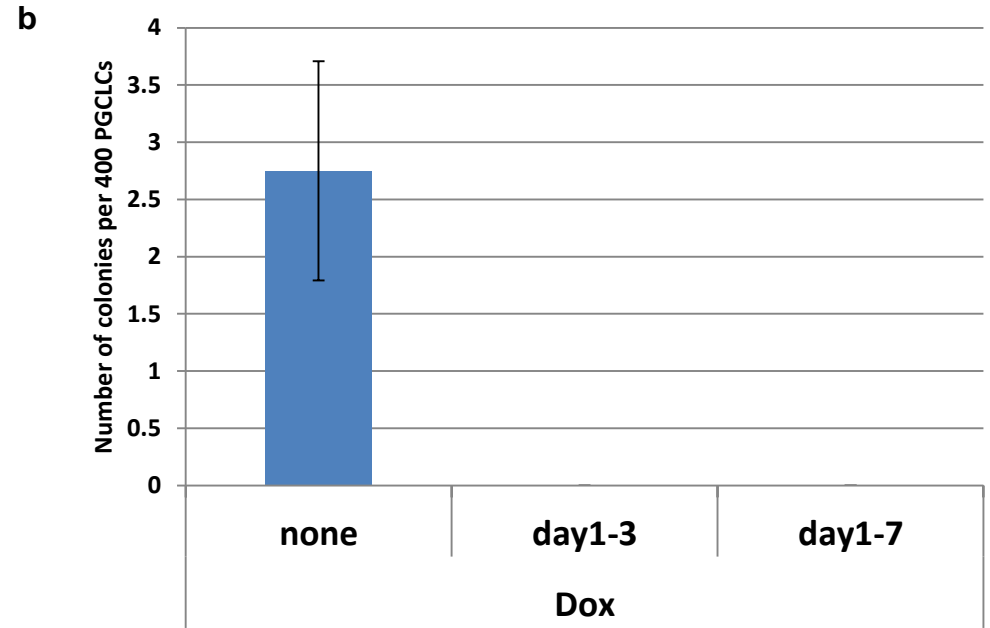
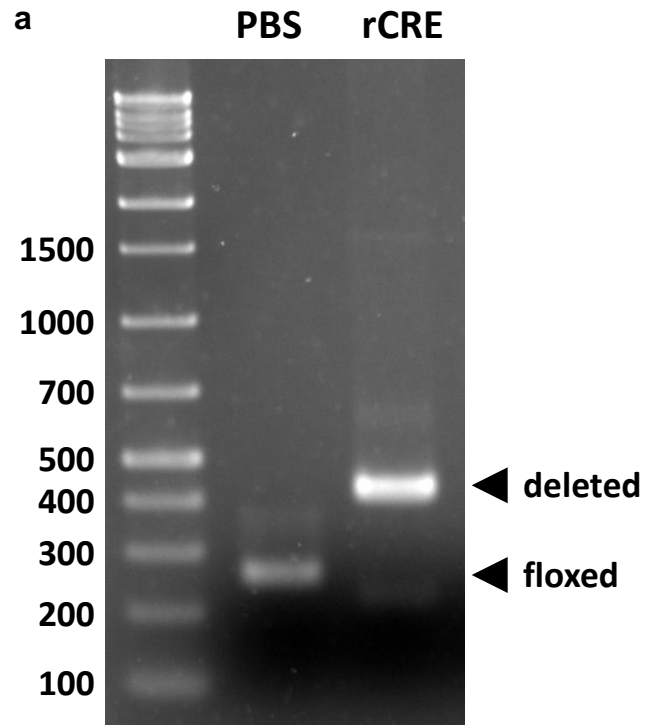


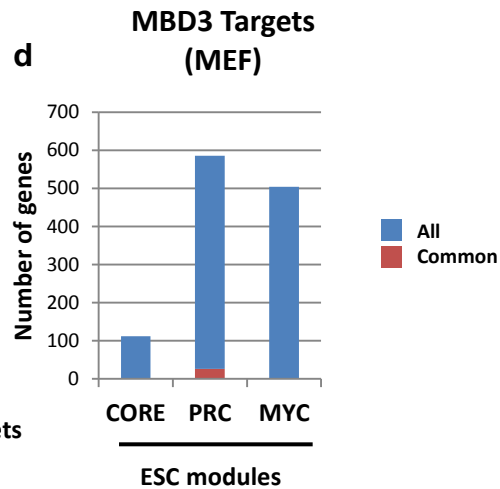
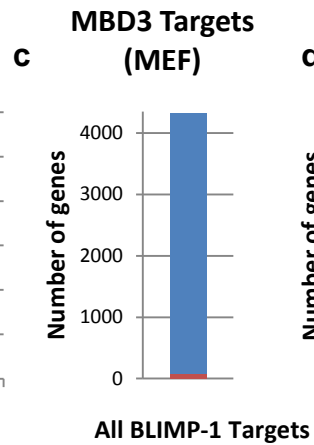
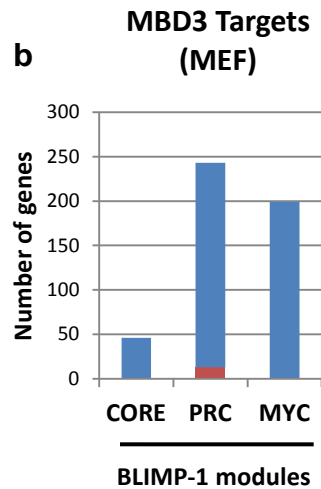
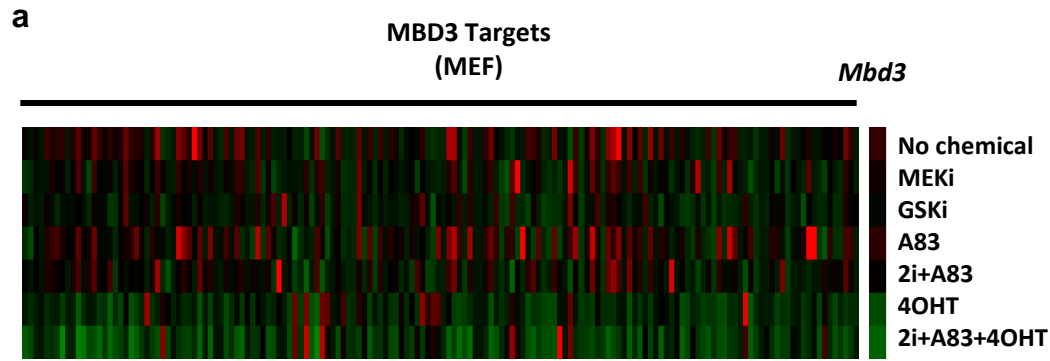
Histone Modification



DNA Methylation







e MBD3 expression in *Akt-mer* MEF

